Bis-Picolinamide ruthenium (III) dihalide complexes: dichloride to diiodide exchange generates single *trans* isomers with high potency and cancer cell selectivity

Aida M. Basri,[a] Rianne M. Lord,[b] Simon J. Allison,[c] Andrea Rodríguez-Bárzano,[a] Stephanie J. Lucas,[a] Felix D. Janeway,[a] Helena J. Shepherd,[d] Christopher M. Pask,[a] Roger M. Phillips[c] and Patrick C. McGowan[a]*

Abstract: A library of new *bis*-picolinamide ruthenium(III) dihalide complexes of the type RuX_2L_2 (X = Cl or I and L = picolinamide) have been synthesised and characterised. They exhibit different picolinamide ligand binding modes, whereby one ligand is bound (*N,N*) and the other bound (*N,O*). Structural studies reveal a mixture of *cis* and *trans* isomers for the $RuCl_2L_2$ complexes but upon a halide exchange reaction to RuI_2L_2, only single *trans* isomers are present. High cytotoxic activity against human cancer cell lines was observed, with potencies for some complexes similar to or better than cisplatin. Conversion to RuI_2L_2 substantially increased activity towards cancer cell lines by >12-fold. The RuI_2L_2 complexes displayed potent activity against the A2780cis (cisplatin-resistant human ovarian cancer) cell line, with >4-fold higher potency than cisplatin. Equitoxic activity was observed against normoxic and hypoxic cancer cells, indicating the potential to eradicate both the hypoxic and aerobic fractions of solid tumours with similar efficiency. Selected complexes were also tested against non-cancer ARPE-19 cells. The RuI_2L_2 complexes are more potent than the $RuCl_2L_2$ analogues, and also more selective towards cancer cells with a selectivity factor >7-fold.

Introduction

The use of *trans* dihalide ancillary ligands in the design of new anti-cancer drugs, based on the structure of transplatin, has received little attention for many years, due to early studies showing the *trans*-Pt complexes to be inactive due to high kinetic instability.[1] However, in recent years, examples of active *trans*-Pt anti-cancer complexes (**Figure 1**) have been reported.[2–9] In 1993, Coluccia *et al.* substituted the ammine in both cisplatin (**a**) and transplatin (**b**), for imino ether substituents and showed the *trans* geometry (**c**) to have the greatest *in vitro* cytotoxicity against P388 leukemia cells.[2] Kelland *et al.* showed that addition of a benzene ring to transplatin resulted in a *trans* complex, JM335 (**d**), that is >3-fold more active than its *cis* analogue.[4] Unlike transplatin, JM335 produced an increase in inter-strand crosslinking with an increase in drug concentration. Farrell *et al.* synthesised compounds of the type *trans*-$[PtL_2Cl_2]$ (**e**) and showed they are as active as cisplatin against a range of cell lines and are dramatically more active than transplatin.[10] More recently, Sadler *et al.* reported a *trans*-$Pt(N_3)_2(OH)_2(Py)_2$ complex (**f**) which is photo-activated by visible light at 420 nm, and is more potent upon light irradiation.[9]

Figure 1 Previously reported *trans*-Pt complexes **a**-**f**

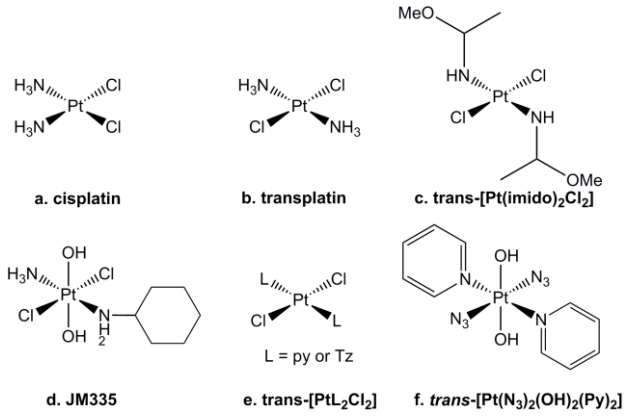

[a] Dr. A. M. Basri, Dr. A. Rodríguez-Bárzano, Dr. S. J. Lucas, Dr. F. D. Janeway, Dr. C. M. Pask and Prof. P. C. McGowan*
School of Chemistry
University of Leeds
Woodhouse Lane, Leeds, LS2 9JT
E-mail*: p.c.mcgowan@leeds.ac.uk
[b] Dr. R. M. Lord
School of Chemistry and Forensic Sciences
University of Bradford
Bradford, BD7 1DP
[c] Dr. S. J. Allison and Prof. R. M. Phillips
School of Applied Sciences
University of Huddersfield
Huddersfield, HD1 3DH
[d] Dr. H. J. Shepherd
School of Physics
University of Kent
Canterbury, Kent, CT2 7NH
Supplementary Information contains X-ray crystallographic data and addition studies. All complexes have been deposited in the Cambridge Crystallographic Data Centre with CCDC references numbers 947781-947791, 1441964-1441970 and 1449661-1449662.

Ruthenium-based complexes are some of the most promising anti-cancer drugs, with reported selective potency *in vitro* and *in vivo* (**Figure 2**).[11,12] However, there has been a lack of suitable *trans* ruthenium derivatives due to the propensity of the molecules to undergo isomerisation. The first reported cytotoxic *trans*-ruthenium complexes were KP1019 (**g**)[13–15] and NAMI-A (**h**),[16–19] which in Phase I clinical trials were well tolerated showing only limited side effects.[20,21] NAMI-A has also undergone Phase II clinical studies in combination with gemcitabine, however, this combination had some adverse toxicity and failed to show any improvement in results compared to gemcitabine treatment alone.[22,23] The activity of NAMI-A is likely to involve multiple mechanisms. At a physiological pH of 7.4 it can undergo hydrolysis leading to release of chloride and DMSO and the formation of a number of potentially active species.[19,24–26] The activity of NAMI-A is also influenced by its redox status. Reduction of NAMI-A strongly depends on pH and is accelerated on increasing the pH resulting in the generation of active Ru(II) product(s).[27] Amongst potential intracellular targets, reduced NAMI-A binds human serum albumin.[28] Unlike cisplatin, DNA is not the main pharmacological target for NAMI-A, although it has been reported that this complex can bind to DNA and inhibit DNA replication *in vitro*.[29,30] KP1019 is thought to be reduced *in vivo* to an active Ru(II) species and also offers a different mode of action to cisplatin, with increased selectivity.[21,31] KP1019, like NAMI-A, also reacts with human serum proteins, including human albumin and transferrin.[32,33] KP1339 (**i**), the sodium salt of KP1019, has better solubility that KP1019[34,35] and has shown promising results in both Phase I and II clinical trial.[36,37] More recently new ruthenium-nitrosyl complexes of the type (H_2ind)[$RuCl_4$(NO)(Hind)] (**j**) were reported, in which both the *cis* and *trans* isomers exhibit time-dependent responses against human cancer cell lines.[38,39] with the *trans*-isomer displaying higher anti-proliferative activity than the analogous *cis*-isomer.

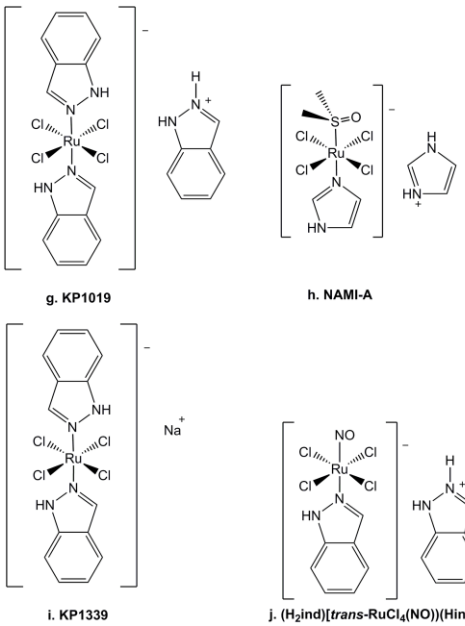

Figure 2 Previously reported trans-ruthenium complexes **g**-**j**

Ruthenium complexes of the type RuX_2L_2 (X = halide, and L = bidentate ligand) were seen previously to undergo isomerisation, giving rise to six different structural geometries (**Figure 3**), this

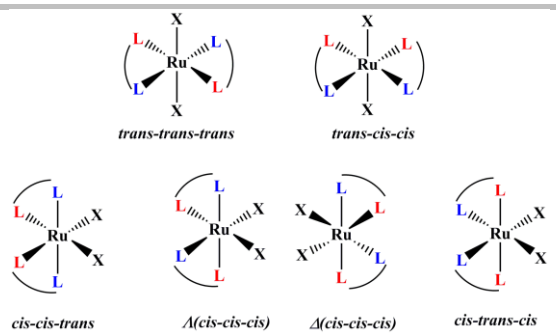

includes the *cis-cis-cis* enantiomer.[40] Reedijk *et al.* have reported the anti-cancer activities of $Ru(azpy)_2Cl_2$ complexes with differences in their activities due to different structural isomers. The *trans* geometries were found to have very low cytotoxicity against a series of cancer cell lines.[41,42] More recently, Glazer *et al.* has compared the activities of *cis*-$Ru(bpy)_2Cl_2$ with *trans*-$Ru(qpy)Cl_2$, showing the *trans* isomer to be 7-10 times more active than the *cis*.[43] This propensity for the formation of different isomers is one of the reasons that there has been much effort dedicated to the synthesis and development of transition metal based candidates that are based on the molecular architecture associated with M-arene,[44–51] MCp*,[47,52–57] and ferrocene derivatives.[58,59]

Figure 3 Possible structural isomers for ruthenium complexes of the type RuX_2L_2; enantiomers for *cis-cis-cis* structure are also shown.

The complexation of ruthenium with picolinamide ligands is of interest because of its relevance to previously reported metal-ion peptide chemistry, and the possibility of different ligand binding modes that can potentially alter the biological activity of the complexes.[60–68] These ligands are able to bind to the metal center either *via* the monoanionic (*N,N*) or (*N,O*) donors through loss of the amide proton, or as neutral (*N,O*) donors.[68,69] Different coordination modes of metal functionalised amide complexes have been shown to affect the activity towards cancer cells.[70–72] The different coordination modes of picolinamide derivatives have also been shown to dramatically affect the potencies of the compound.[50] The (*N,N*) bound complexes undergo rapid hydrolysis, bind with guanine and are cytotoxic to cancer cells, whereas the (*N,O*) bound complexes showed low activity and undergo slow hydrolysis. Herein we report on the synthesis and evaluation of a library of new ruthenium complexes of the type RuX_2L_2 (X = Cl or I, and L = bidentate functionalised picolinamide ligands), whereby one ligand coordinates (*N,N*) and the second ligand coordinates (*N,O*) to the ruthenium metal center. The synthesis of such complexes follows a known synthetic procedure by Chan *et al.*,[73] in which the complex **6** reported here was assessed as a potential catalyst for the epoxidation of cyclic alkenes. Bhattacharya *et al.* has also synthesised similar complexes consisting of one or three picolinamide (L) ligands, [Ru(L)(PPh_3)(H)(CO)] and [$Ru(L)_3$] respectively with the ligands all bound (*N,N*) to the ruthenium metal center.[68,74]. We report on halide exchange reactions to yield the *bis* iodide complexes, [$RuI_2(L)_2$], which give single *trans* isomers, thus potentially minimising any future drug formulation issues due to the presence of multiple isomers with different effects or potency. These complexes have been measured in both solid state and solution in order to identify the potential isomers present. The *trans*

isomers show surprisingly high cytotoxicity, with IC_{50} values in the nanomolar range, and high selectivity towards cancer cells.

Results and Discussion

Synthesis of *Bis*-Picolinamide Ruthenium(III) Dihalide Complexes

The picolinamide ligands were synthesised *via* a known literature preparation, from picolinic acid and a functionalised aniline.[58] Compounds **1**-**16** were prepared by reacting $RuCl_3.3H_2O$ with two equivalents of functionalised picolinamide ligand and heating at reflux for 2 hours in ethanol, in the presence of one equivalent of triethylamine (**Scheme 1a**). Complex **6** has previously been reported by Chan *et al.*[73] and was synthesised for pairwise comparison with its diiodide analogue, and to complete our library of RuX_2L_2 structures. Compounds **17**-**31** were synthesised by a halide-exchange reaction of the ruthenium dichloride complexes with an excess of KI, by refluxing in ethanol overnight (**Scheme 1b**).[75,76] We have analysed the IR spectra of the picolinamide ligand precursors and the ruthenium dihalide complexes, which also verified successful complex synthesis. The spectra show CO and NH stretches for the ligand precursor at ~1690 cm^{-1} and ~3300 cm^{-1} respectively. Upon complexation, these peaks were shifted to lower wavenumbers of ~1590 cm^{-1} and ~3060 cm^{-1} respectively, for both the $RuCl_2L_2$ and RuI_2L_2 complexes. Magnetic susceptibility measurements also confirmed all the ruthenium dihalide complexes to be in the +3 oxidation state and low-spin d^5 with one unpaired electron (μ_{eff} = 1.60-2.53 μ_B).

Structural Characterisation

Six structural isomers are possible for complexes of the type RuX_2L_2, as shown in **Figure 3**.[77] The $RuCl_2L_2$ complexes gave red single crystals from vapor diffusion of pentane into methanol or hexane into methanol, and black/green single crystals for the RuI_2L_2 complexes which were obtained from vapor diffusion of diethyl ether into DMF. The molecular structures for $RuCl_2L_2$ complexes **1**, **3**, **5**-**7**, **9**, **11**-**13** and **15**-**16**, and for RuI_2L_2 complexes **18**, **19**, **28** and **29**, as determined by X-ray crystallography, are presented in **Figure 4a-b** and **Figure 5** respectively. Complex **6** was previously reported as the *cis(X)-cis(N,N)-trans(N,O)* conformer,[73] however, here we crystallised the complex as the *cis(X)-cis(N,N)-cis(N,O)* conformer. Selected bond lengths and angles are stated in **Tables 1** and **2** for $RuCl_2L_2$ complexes and **Table 3** for RuI_2L_2 complexes. The X-ray crystallography data is detailed in the **Tables S3-S5** (*Supplementary Information*). The picolinamide ligands bind to the ruthenium metal center in a *(N,N)* and *(N,O)* bidentate fashion, as confirmed by their crystal structures, giving a ruthenium complex with a +3 oxidation state. Upon recrystallisation of complexes **1**, **7** and **16**, different crystal morphologies were observed in the crystallisation vials. X-ray crystallographic analysis of the different morphologies confirmed that these complexes co-crystallise as a mixture of isomers, and their structures are shown in **Figures 4a** and **4b** Three different types of structural isomer were observed for the $RuCl_2L_2$ complexes, the *cis(X)-cis(N,N)-cis(N,O)* (**1a**, **6**, **7a** and **12**), *cis(X)-trans(N,N)-cis(N,O)* (**15** and **16a**) and *trans(X)-trans(N,N)-trans(N,O)* (**1b**, **3**, **5**, **7b**, **9**, **11**, **13** and **16b**) arrangements. Due to the larger ionic radius of iodine and potential structural constraints around the ruthenium metal center posed by this, we hypothesised that the ruthenium iodide complexes might lead to fewer structural isomers than their dichloride analogues (**Scheme 1**). Indeed, the crystal structures of RuI_2L_2 complexes **18**, **19**, **28** and **29** revealed a stable *trans(X)-trans(N,N)-trans(N,O)* (**Figure 5**). The *bis*-picolinamide ruthenium dihalide complexes have typical M-X bond lengths and bond angles which are characteristic of a distorted octahedral geometry (**Table 1** and **2** for $RuCl_2L_2$ and **Table 3** for RuI_2L_2).

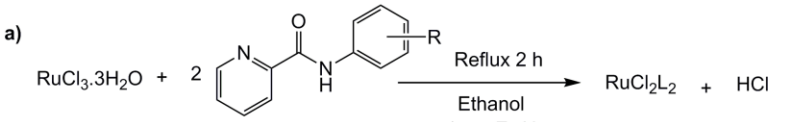

R	X = Cl	X = I	R	X = Cl	X = I
H	**1** (74%)	**17** (58%)	2',4'-diCl	**9** (44%)	**25** (44%)
2'-F	**2** (50%)	**18** (59%)	2',5'-diCl	**10** (40%)	**26** (44%)
4'-F	**3** (52%)	**19** (58%)	2'-Br	**11** (46%)	**27** (52%)
2',4'-diF	**4** (72%)	**20** (36%)	3'-Br	**12** (62%)	**28** (50%)
2',5'-diF	**5** (28%)	**21** (31%)	4'-Br	**13** (44%)	**29** (52%)
2'-Cl	**6** (58%)	**22** (34%)	2',4'-diBr	**14** (51%)	**30** (74%)
3'-Cl	**7** (55%)	**23** (62%)	2',5'-diBr	**15** (54%)	**31** (33%)
4'-Cl	**8** (28%)	**24** (60%)	2'-I	**16** (34%)	

Scheme 1 Synthetic pathways of **a)** $RuCl_2L_2$ and **b)** RuI_2L_2 complexes, showing the yields for different R and X substituents.

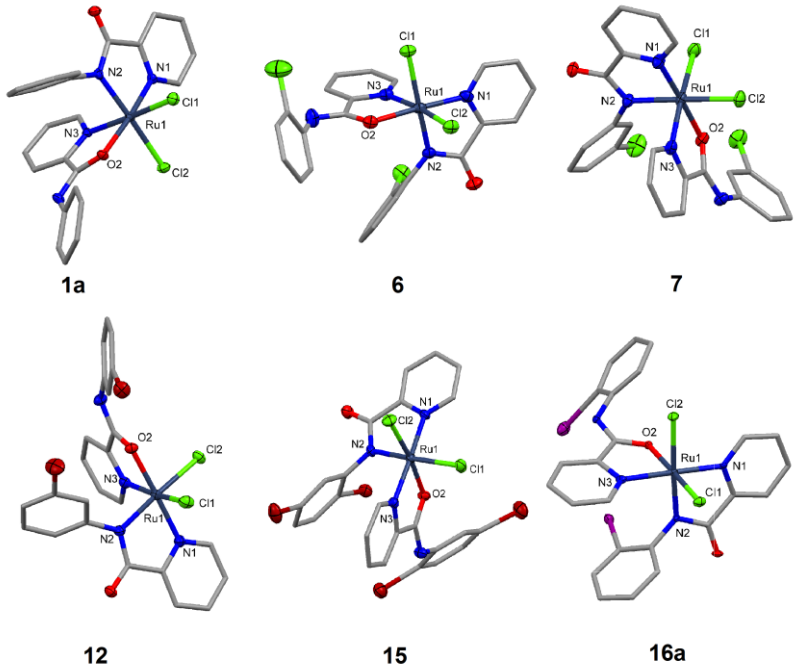

Figure 4a Molecular structures of $RuCl_2L_2$ complexes **1a**, **6**, **7a** and **12** showing *cis(X)-cis(N,N)-cis(N,O)* arrangements and **15** and **16a** showing *cis(X)-trans(N,N)-cis(N,O)* arrangements. Hydrogen atoms and solvent molecules are omitted for clarity and displacement ellipsoids are at the 50% probability level (shown only for the heteroatoms).

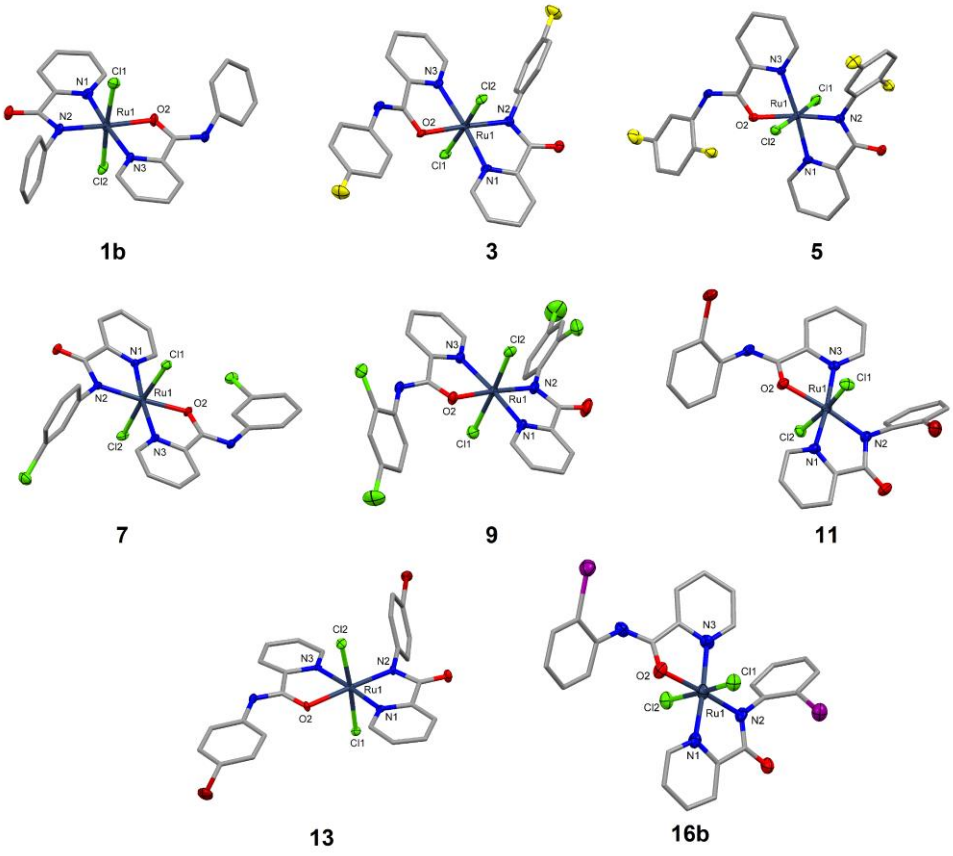

Figure 4b Molecular structures of $RuCl_2L_2$ complexes **1ᵇ**, **3**, **5**, **7ᵇ**, **9**, **11**, **13** and **16ᵇ** all showing *trans(X)-trans(N,N)-trans(N,O)* arrangements. Hydrogen atoms and solvent molecules are omitted for clarity and displacement ellipsoids are at the 50% probability level (shown only for the heteroatoms).

Table 1 Bond lengths (Å) and bond angles (°) for $RuCl_2L_2$ *cis(X)-cis(N,N)-cis(N,O)* complexes **1**[a], **6**, **7**[a] and **12**, and *cis(X)-trans(N,N)-cis(N,O)* complexes **15**-**16**[a]

Bond length (Å)	**1**[a]	**6**	**7**[a]	**12**	**15**	**16**[a]
Ru1-Cl1	2.3540(9)/	2.345(2)	2.3594(6)	2.3505(7)	2.3462(10)	2.3241(13)
Ru1-Cl2	2.3769(9)	2.381(3)	2.3848(5)	2.3833(7)	2.3943(10)	2.3600(13)
Ru1-N1	2.018(3)	2.030(8)	2.0510(15)	2.053(2)	2.089(3)	2.045(4)
Ru1-N2	1.997(3)	2.013(8)	2.0270(14)	2.029(2)	2.052(3)	2.030(4)
Ru1-N3	2.045(3)	2.071(8)	2.0741(16)	2.080(2)	2.096(3)	2.060(4)
Ru1-O2	2.087(3)	2.091(7)	2.1089(12)	2.1043(17)	2.113(2)	2.056(3)
Bond angle (°)	**1**[a]	**6**	**7**[a]	**12**	**15**	**16**[a]
Cl1-Ru1-Cl2	96.16(3)	95.39(9)	95.033(19)	95.57(2)	94.71(4)	92.54(5)
N1-Ru1-O2	175.63(10)	176.8(3)	177.80(6)	178.36(8)	98.88(10)	93.55(14)
N2-Ru1-O2	96.34(11)	97.1(3)	98.13(5)	98.69(8)	85.17(10)	91.98(14)
N2-Ru1-N3	86.23(11)	87.7(3)	88.07(6)	87.81(8)	97.05(11)	94.94(15)
N1-Ru1-N3	98.72(11)	100.8(3)	100.49(6)	102.07(8)	175.62(11)	171.69(15)

Table 2 Bond lengths (Å) and bond angles (°) for $RuCl_2L_2$ *trans(X)-trans(N,N)-trans(N,O)* complexes **1**[b], **3**, **5**, **7**[b], **9**, **11**, **13** and **16**[b]

Bond length (Å)	**1**[b]	**3**	**5**	**7b**	**9**	**11**	**13**	**16**[b]
Ru1-Cl1	2.3408(14)	2.3318(10)	2.3328(9)	2.3355(9)	2.3543(6)	2.3452(9)	2.3397(13)	2.330(4)
Ru1-Cl2	2.3498(13)	2.3533(10)	2.3664(9)	2.3362(9)	2.3767(5)	2.3914(8)	2.3425(14)	2.352(3)
Ru1-N1	2.037(4)	1.999(3)	2.036(3)	2.033(3)	2.0514(15)	2.056(3)	2.039(4)	2.023(13)
Ru1-N2	2.008(4)	2.036(3)	2.027(3)	2.006(3)	2.0273(15)	2.036(3)	1.996(4)	2.016(10)
Ru1-N3	2.102(4)	2.113(3)	2.102(3)	2.106(3)	2.1219(15)	2.106(3)	2.089(4)	2.067(12)
Ru1-O2	2.067(3)	2.087(3)	2.077(2)	2.061(2)	2.1056(13)	2.095(2)	2.100(4)	2.116(9)
Bond angle (°)	**1**[b]	**3**	**5**	**7b**	**9**	**11**	**13**	**16**[b]
Cl1-Ru1 Cl2	175.93(5)	176.60(5)	176.80(3)	174.66(3)	173.54(18)	174.27(3)	176.59(5)	173.82(13)
N1-Ru1-O2	96.51(16)	97.82(16)	95.46(11)	96.70(10)	96.08(6)	96.76(10)	97.83(16)	98.3(4)
N2-Ru1-O2	175.18(16)	176.38(16)	174.21(10)	175.10(10)	175.25(6)	174.07(10)	176.41(16)	176.3(5)
N2-Ru1-N3	106.92(16)	105.90(18)	107.74(11)	107.74(11)	106.95(6)	106.13(11)	105.86(18)	104.6(5)
N1-Ru1-N3	174.22(16)	175.45(18)	173.36(11)	173.84(10)	173.80(6)	174.43(11)	175.47(18)	175.8(5)

Powder X-ray Diffraction

Powder diffraction studies were carried out on both $RuCl_2L_2$ and RuI_2L_2 compounds, using both the bulk sample and single crystals. The diffractogram obtained for the $RuCl_2L_2$ complex **7** was overlaid with both the simulated *cis* and simulated *trans* geometries, and shows that in the bulk sample, multiple isomers are present (**Figure 6**), which correlated well with the observed multiple morphologies in the crystallisation vials.

Powder diffraction studies on the RuI_2L_2 complex **18** for both simulated and single crystals were analysed and show the bulk powder sample contains only a single stable *trans* geometry (**Figure 7**, **black**). This result is consistent with the crystal morphology observed in the crystallization vial, whereby only *trans* isomers of the RuI_2L_2 complexes were isolated. The simulated pattern for the *trans* geometry is the same as the single crystal structure and indicates that the RuI_2L_2 complex only exists as a single *trans* geometry in solid-state.

Complex isomerisation during the formulation of drugs is a key issue as different isomers can potentially have different therapeutic effects, single isomer synthesis is therefore very important. The PXRD results indicate we can synthesise the RuI_2L_2 complexes as single *trans* isomers thereby satisfying this key requirement, and highlighting the potential progression of compound towards further clinical trials.

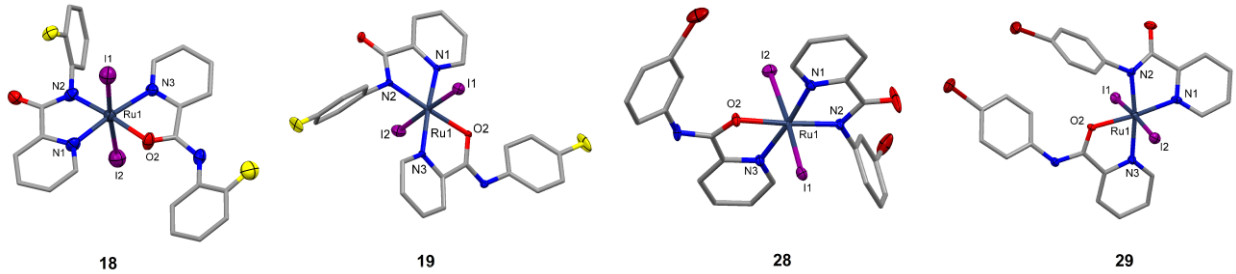

18 **19** **28** **29**

Figure 5 Molecular structures of RuI_2L_2 complexes **18**, **19** and **28** showing *trans(X)-trans(N,N)-trans(N,O)* arrangements and **29** showing a *trans-cis-cis* arrangement. Hydrogen atoms and solvent molecules are omitted for clarity and displacement ellipsoids are at the 50% probability level (shown only for the heteroatoms).

Table 3 Bond lengths (Å) for RuI_2L_2 *trans(X)-trans(N,N)-trans(N,O)* complexes **18**, **19**, **28** and **29**

Bond length (Å)	**18**	**19**	**28**	**29**
Ru1-I1	2.6507(17)	2.6589(8)	2.701(4)	2.664(11)
Ru1-I2	2.6670(18)	2.7149(8)	2.703(4)	2.685(11)
Ru1-N1	2.031(13)	2.051(6)	2.065(3)	2.039(7)
Ru1-N2	2.009(11)	2.021(6)	2.023(3)	2.023(7)
Ru1-N3	2.123(12)	2.119(6)	2.122(3)	2.118(7)
Ru1-O2	2.106(10)	2.089(5)	2.092(3)	2.066(6)
Bond angle (°)	**18**	**19**	**28**	**29**
I1-Ru1-I2	174.89(6)	177.93(3)	174.3 (14)	174.1(4)
N1-Ru1-O2	97.1(4)	96.6(2)	96.85(12)	174.9(3)
N2-Ru1-O2	175.4(5)	174.3(2)	175.56(13)	96.2(3)
N2-Ru1-N3	107.2(5)	107.4(2)	107.41(12)	171.6(3)
N1-Ru1-N3	173.7(5)	173.7(2)	173.65(13)	108.0(3)

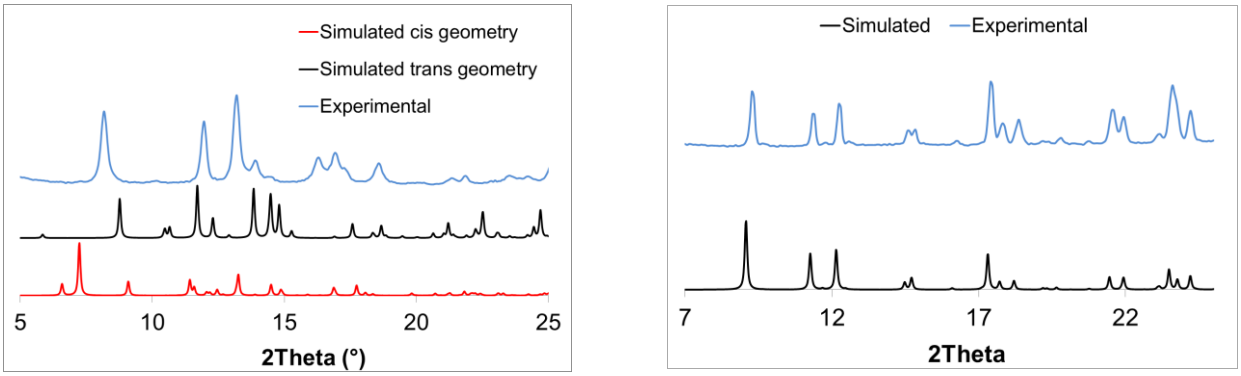

Figure 6 Powder X-ray diffractograms for $RuCl_2L_2$ complex **7**, showing simulated *cis* or *trans* geometry (**red** and **black**) and experimental data (**blue**).

Cell Line Chemosensitivity Studies

The *bis*-picolinamide ruthenium(III) dihalide complexes were tested for their cytotoxicity against three human cancer cell lines, A2780 (human ovarian cancer), A2780*cis* (cisplatin- resistant human ovarian cancer) and HT-29 (human colorectal cancer).

Figure 7 Powder X-ray diffractograms of RuI_2L_2 complex **18** showing simulated *trans* geometry (**blue**) and experimental data (**black**).

To assess selectivity towards cancer cells, cytotoxicity towards an epithelial non-cancer cell line (ARPE-19) was also determined. The IC_{50} values for these compounds and cisplatin, which is in clinical use for treatment of human ovarian cancer, are shown in **Table 4**.

Table 4 Response of A2780, A278cis, HT-20 and ARPE-19 cell lines to complexes **1**-**31** and cisplatin. Each value represents the mean (± standard deviation) of at least 3 independent experiments.

		IC_{50} values / μM ± SD							
Compound		A2780		A2780cis		HT-29		ARPE-19	
Cisplatin		1.4 ± 0.3		11 ± 0.6		2.8 ± 0.3		5.97 ± 0.95[15e]	
X = Cl	X = I	X = Cl	X = I	X = Cl	X = I	X = Cl	X = I	X = Cl	X = I
1	**17**	24 ± 2	5.4 ± 0.5	47 ± 3.0	5.3 ± 0.2	23.0 ± 0.4	5.5 ± 0.4		2.8 ± 0.2
2	**18**	13 ± 1	13.0 ± 0.6	21 ± 1.8	31 ± 2	6.2 ± 0.4	13.0 ± 0.9		
3	**19**	6.9 ± 0.8	3.4 ± 0.1	35 ± 3	12.0 ± 0.5	17 ± 1	8.4 ± 0.3	17.9 ± 0.1	6.3 ± 0.3
4	**20**	22 ± 1	14 ± 1	25.0 ± 0.6	13.0 ± 0.4	7.3 ± 0.4	8.5 ± 0.7	30 ± 2	26 ± 4
5	**21**	45 ± 2	16.0 ± 0.3	93 ± 2	15 ± 1	20 ± 1	14 ± 2		
6	**22**	21.0 ± 0.4	7.2 ± 0.1	33 ± 1	22 ± 2	11.0 ± 0.5	10 ± 1		
7	**23**	3.6 ± 0.2	2.8 ± 0.3	6.7 ± 0.1	3.2 ± 0.1	3.0 ± 0.1	2.3 ± 0.1		
8	**24**	9.2 ± 0.4	2.5 ± 0.2	4.4 ± 0.4	2.4 ± 0.2	2.8 ± 0.3	0.9 ± 0.1	2.53 ± 0.01	3.42 ± 0.04
9	**25**	41.0 ± 0.7	6.6 ± 0.6	55 ± 2	4.3 ± 0.3	9.7 ± 0.3	3.4 ± 0.3	59 ± 3	11 ± 2
10	**26**	31.0 ± 0.9	10.0 ± 0.4	24 ± 2	12.0 ± 0.4	11.0 ± 0.9	6.5 ±0.3		
11	**27**	18 ± 2	11.0 ± 0.6	37 ± 1	40 ± 2	8.3 ± 0.3	24 ± 2		
12	**28**	3.3 ± 0.2	2.0 ± 0.2	6.0 ± 0.4	3.3 ± 0.1	3.3 ± 0.2	1.5 ± 0.1		
13	**29**	7.5 ± 0.3	2.3 ± 0.2	12.0 ± 0.9	2.9 ± 0.2	6.8 ± 0.3	0.8 ± 0.1	4.85 ± 0.05	2.34 ± 0.02
14	**30**	18.0 ± 0.8	6.7 ± 0.3	26 ± 1	6.6 ± 0.3	7.7 ± 0.3	4.3 ± 0.2	37 ± 7	34 ± 4
15	**31**	20 ± 2	11.0 ± 0.6	22 ± 2	7.6 ± 0.3	10.0 ± 0.6	4.9 ± 0.4		

Against A2780 cancer cells, the unsubstituted picolinamide ruthenium dichloride complex **1** was found to be moderately active with an IC_{50} value of 24 ± 1.6 μM. Addition of a substituent to the phenyl ring of the picolinamide ligands generally increased potency especially when a substituent was placed in the *meta* or *para* position (**Table 4**, complexes **3**, **7**, **8**, **12**, **13**, **23**, **24**, **28** and **29**). The most active ruthenium dichloride complex against A2780 cells was complex **12**, which has a bromide substituent in the *meta* position on the phenyl ring of the picolinamide ligand, with an IC_{50} value of 3.3 ± 0.2 μM, comparable with that of cisplatin (1.4 ± 0.3 μM). The least active is complex **5** which has a 2',5'-difluoro substituent and only a moderate IC_{50} value of 45 ± 2 μM. A similar trend for the ruthenium dichloride complexes was observed against the cisplatin-resistant A2780cis cancer cell line with the exception of fluoride substituents, where *ortho*-fluoro (**2**) was more active than *para*-fluoro (**3**). Complexes **7**, **8** and **12**, which were amongst the most active ruthenium dichloride complexes against the A2780 cancer cells, were all more active than cisplatin against A2780cis cancer cells, with IC_{50} values of 6.7 ± 0.1 μM, 4.4 ± 0.4 μM and 6.0 ± 0.4 μM respectively, compared to an IC_{50} value of 11.0 ± 0.6 μM for cisplatin ($p < 0.01$, for complexes **7**, **8** and **12** compared to cisplatin). Interestingly, *para*-chloro complex **8** was ~2-fold more cytotoxic ($p < 0.01$) towards the cisplatin-resistant A2780cis cancer cells than the A2780 cisplatin-sensitive cells (**Figure 8**).

In addition to complex **8**, complex **10** and ruthenium diiodide complexes **25** and **31** were also more active towards the cisplatin-resistant cells than the parental cisplatin-sensitive A2780 cells (**Figure 8**). Furthermore, many of the ruthenium diiodide complexes were equally active against A2780 and A2780cis cells (complexes **17**, **20**, **21**, **24** and **30**) than the corresponding ruthenium dichloride complexes (**Figure 8**). There are currently only a few organometallic complexes that have been shown to

overcome mechanisms of cisplatin resistance in cancer cells.[78–80] These results suggest that these complexes may be able to circumvent cisplatin resistance mechanisms in ovarian cancer cells,[81–84] which is a critical goal in developing new organometallic complexes with high cytotoxic activity against cancer cell lines.

Against HT-29 cells, complexes **1**, **7**, **12**, and **13** showed very similar activity to that observed against the A2780 cancer cells. However, the majority of ruthenium dichloride complexes were significantly more active against HT-29 cells. For example, complex **9** showed poor activity against A2780 cells (IC_{50} = 41.0 ± 0.7 μM) but was approximately 4-fold more active (p < 0.01) against HT-29 cells (IC_{50} = 9.7 ± 0.3 μM). Further studies are required but this suggests that some of the complexes may have preferential activity towards certain cancer cell types. The least active complex against HT-29 cells was unsubstituted complex **1,** with the addition of a *para* or *meta* substituent on the phenyl ring of the picolinamide ligand, the compounds generally increase in cytotoxicity.

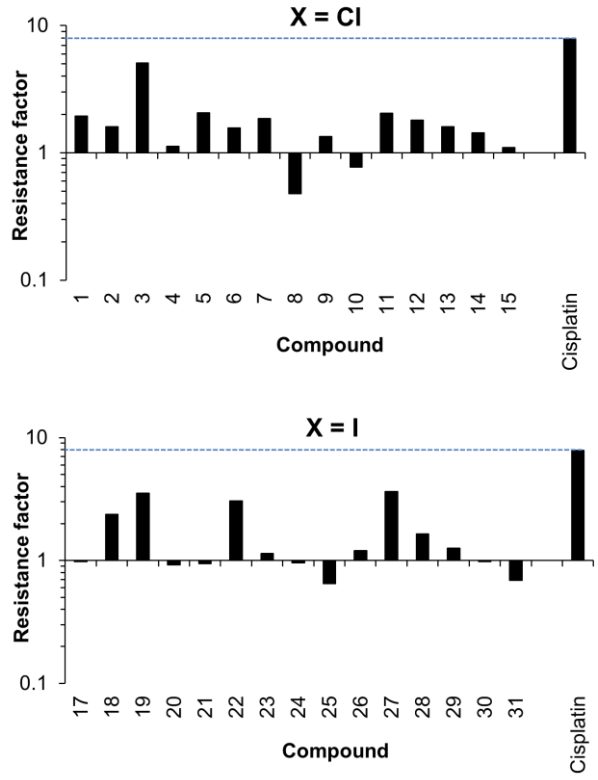

Figure 8 Response of A2780 and A2780cis cells to complexes **1**-**31** and cisplatin. The results are expressed as the resistance factor defined as the ratio of the mean IC_{50} for A2780cis divided by the mean IC_{50} for A2780 cells. Values > 1 indicate that the complex is less cytotoxic towards A2780cis cells than A2780 parental cells whereas values = 1 indicate that complexes are as active against A2780 and A2780cis cells. Values < 1 indicate that complexes are preferentially active against cisplatin resistant A2780cis cells

The effects of converting ruthenium dichloride to diiodide were also compared for each of the fifteen different picolinamide complexes (**Table 4**). Unexpectedly, replacement of ruthenium dichloride with diiodide resulted in remarkably higher potency for most of the complexes and this was observed against all three human cancer cell lines tested (**Figure 9**). The ruthenium dichloride complex **9** (R = 2',4'-Cl) is one of the least cytotoxic in the series, and substitution of dichloride with diiodide increases the IC_{50} values >12-fold. Against cisplatin-resistant A2780cis cancer cells, over half of the diiodide complexes were more active than cisplatin. In particular, compounds **23**, **24**, **28** and **29**, were particularly potent with IC_{50} values of 2.4-3.3 μM compared to 11 μM for cisplatin. Against all three cancer cell lines, diiodide complexes **24** (4'-Cl) and **29** (4'-Br) were highly potent with >4-fold higher cytotoxicity against the A2780cis cancer cells than cisplatin, and show nanomolar potency towards HT-29 cancer cells (**Table 4**).

Selectivity Towards Cancer Cells

A major limitation of many existing anti-cancer drugs is poor selectivity towards cancer cells. This restricts the drug dosage that can be used and thus effectiveness of treatment, as well as resulting in harmful side effects for the patient. Here we have

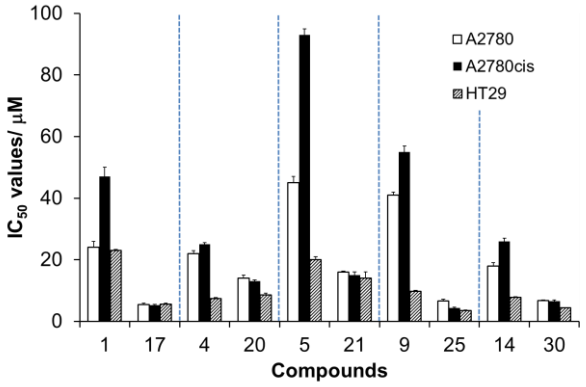

Figure 9 Bar-chart showing the decrease in IC_{50} values and an increase in potency against A2780, A2780cis and HT-29 cell lines, on conversion from the ruthenium dichloride to the diiodide complex (**1** vs **17**; **4** vs **20**; **5** vs **21**; **9** vs **25** and **14** vs **30**). The broken lines represent Cl/ I pairs of compounds.

compared the responses of cancer cells and non-cancer ARPE-19 cells, to a subset of the complexes to obtain a preliminary indication of their cancer selectivity (**Figure 10**; complexes **3**, **4**, **8**, **9**, **13**, **14**, **17**, **19**, **20**, **24**, **25**, **29** and **30**). The results are expressed as the selectivity index defined as the ratio of the mean IC_{50} for the normal ARPE-19 cells (**Table 4**) divided by the mean IC_{50} for each individual cancer cell line tested **Table 4**) with values > 1 indicating selectivity for cancer cells *in vitro*.

Strikingly, with the exception of complex **3** *versus* complex **19**, a general trend was seen whereby the ruthenium diiodide complexes showed *increased cancer selectivity* than their dichloride analogues as well as *higher potency*. The effects of ruthenium dichloride *versus* diiodide (compare paired compounds, **3** vs **19**; **4** vs **20**; **8** vs **24**; **9** vs **25**; **13** vs **29** and **14** vs **30**) and other substitutions on selectivity are shown in **Figure 10** (top panel X = Cl versus bottom panel X = I). Ruthenium dichloride complexes **8** and **13** and unsubstituted ruthenium diiodide complex **17** were more cytotoxic towards the non-cancer ARPE-19 cells than towards the three cancer cell lines as indicated by selectivity ratios <1. In contrast, ruthenium dichloride complexes **4**, **9**, and **14** and ruthenium diiodide complexes **20**, **24**, **25**, **29** and **30** all showed good cancer selectivity with selectivity indices against HT-29 cancer cells ranging from 2.8-fold up to 7.8-fold. Ruthenium diiodide complexes **20**, **25** and **30** showed good

selectivity towards the cisplatin-resistant A2780 cancer cells, with selectivity ranging from 2 to 5-fold increased chemosensitivity towards the cisplatin- resistant cancer cells compared to that for the healthy non-cancer cells.

When comparing the ruthenium diiodide (X = I) and ruthenium dichloride (X = Cl) complexes, on substituting R = 4'-F/Cl/Br with R = 2',4'-diF/diCl/diBr a general reduction in potency towards the cancer cell lines was observed (**Table 4**). However, interestingly, these substitutions reduced activity towards the non-cancer ARPE-19 cells to a greater extent. The consequence of this is that substitution of R = 4'-F/Cl/Br with R = 2',4'-diF/diCl/diBr (**3** vs **4**; **8** vs **9**; **13** vs **14**; **19** vs **20**; **24** vs **25** and **29** vs **30**) generally increased cancer cell selectivity as indicated by a higher selectivity index (**Figure 10**). For example, complex **30** with a 2',4'-dibromo substitution showed 2.8 to 6.3-fold higher cancer selectivity against all cell lines compared to 4'-bromo substituted complex **29** (**Figure 10**).

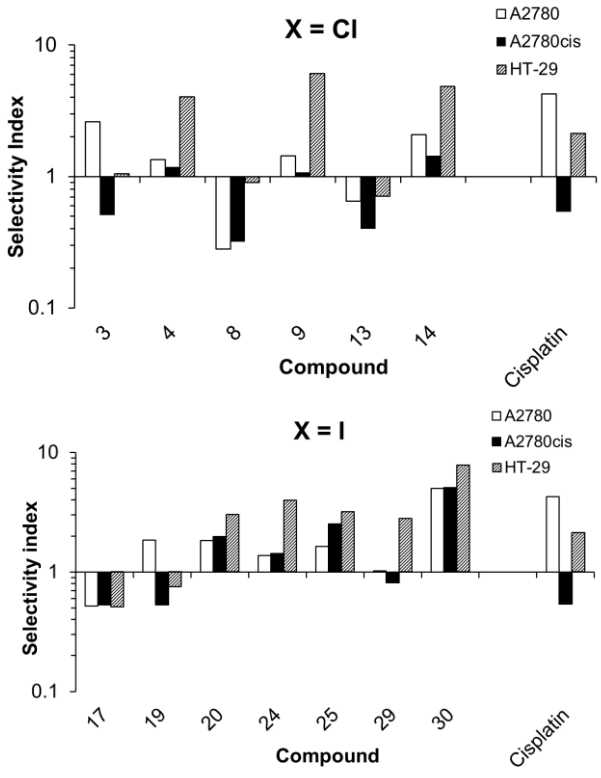

Figure 10 Response of human cancer cell lines compared to non-cancerous ARPE-19 cells. The results are expressed in terms of a selectivity index defined as the ratio of mean IC_{50} values for ARPE-19 cells divided by the IC_{50} for each tumour cell line. Values >1 indicate that complexes are selectivity cytotoxic to cancer cells as opposed to ARPE-19 cells.

Based upon their potency, selective activity and lack of cross resistance with cisplatin, diiodide complexes **25** and **30** appeared particularly promising as potential lead compounds and were further analysed for their activity with very short cellular exposure times (**Table S7**, *Supplementary Information*). Whilst complexes **25** and **30** showed very similar activity against HT29 cells with 5 days continuous exposure (3.4 vs 4.3µM), notable differences were observed with short drug exposure times. With 1, 3 and 6 hours drug exposure times, complex **30** was consistently the more active with an IC_{50} of 30 µM for 1h exposure decreasing to 20 µM for 6 h exposure compared to an IC_{50} of 49 µM for complex **25**. Whilst there are number of possible reasons for these differences, this indicates the need for future further pharmacological evaluation of the most promising compounds.

Chemosensitivity Under Hypoxic Conditions

Due to poor and chaotic tumour vasculature, a proportion of the cancer cells within a solid tumour are in a hypoxic (low oxygen) environment.[85] These cancer cells are typically more resistant to chemotherapy[86] and there is a pressing need for new anti-cancer drugs whose activity is not adversely affected by hypoxia.[85,87] To assess the impact of hypoxia on the potency of these novel *bis*-picolinamide ruthenium complexes, the cytotoxicity of several of the complexes were compared for HT-29 colorectal cancer cells growing under normal oxygen conditions *versus* under hypoxia (0.1% O_2). The two most potent ruthenium dichloride (**7**, **12**) and diiodide (**24**, **29**) complexes were selected activity assess towards cells in hypoxic conditions. **Table 5** shows the normoxic and hypoxic IC_{50} values against HT-29 cells for complexes **7**, **12**, **24** and **29**, along with, tirapazamine (TPZ), a hypoxia-activated drug,[88] which was used to validate the hypoxic conditions. As expected, TPZ was significantly more active under hypoxic conditions than normoxia. All four of the dihalide complexes tested retained their potency under hypoxic conditions with very similar activity observed under normoxic and hypoxic conditions. For complexes **24** and **29** a slight increase in IC_{50} values up to 1.3 µM was observed but this was found to be statistically insignificant ($p > 0.05$). Whilst none of the complexes showed preferential activity towards hypoxic cells, importantly, the equitoxic activity observed indicates that these complexes could potentially be used to target both the hypoxic and aerobic fractions of solid tumours with similar efficiency.

Table 5 Response of HT-20 cells to compounds **7**, **12**, **24**, **29** and TPZ, under normoxic and hypoxic conditions.

Compound	IC_{50} values / µM ± SD		
	Normoxia, 21% O_2 level	Hypoxia, 0.1% O_2 level	Hypoxic cytotoxicity ratio
Tirapazamine	33.0 ± 2.0	2.8 ± 0.4	11.8
Cisplatin	2.8 ± 0.1	2.4 ± 0.3	1.2
7	3.0 ± 0.1	2.6 ± 0.3	1.2
12	3.3 ± 0.2	3.9 ± 0.2	0.8
24	0.86 ± 1.2	1.2 ± 0.2	0.7
29	0.84 ± 1.3	1.3 ± 0.1	0.6

Impact of Hydrolysis on Biological Activity

The cytotoxicity of cisplatin,[89–92] is dependent on its hydrolysis,[93] however recent computation studies suggest no involvement of *cis*-$[Pt(NH_3)_2(OH_2)_2]^{2+}$ and *cis*-$[Pt(NH_3)_2(OH_2)(OH)]^{+}$ in the mode of action of the drug.[94] As discussed previously, the modes of action of both NAMI-A and KP1019 are thought to be due to the reduction of Ru(III) to Ru(II).[24,27] However, ruthenium "piano-stool" complexes with ancillary halide ligands have been shown to hydrolyse and bind to nucleobases bases,[50,95,96] in which the intermediate is thought to be a cationic di-hydrated or mono-

hydrated species under physiological conditions. The hydrolysis potential has been assessed here for both $RuCl_2L_2$ and RuI_2L_2 complexes, in which both the di-hydrated or mono-hydrated species could form (**Scheme 2**).[97,98]

Scheme 2 Proposed hydrolysis scheme of the *bis*(picolinamide) ruthenium(III) dichloride complexes to cationic mono- and di-aquated intermediates.

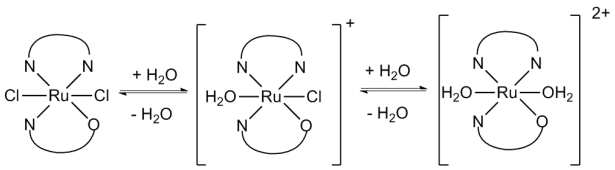

Compounds **3**, **5**, **7**, **10**, **12** and **14** were analysed in aqueous solutions as these represent some of the most active ruthenium dichloride complexes (**7**, **12**) and some of the least active (**5**, **10**) across the cell lines tested. ES-MS analysis of compounds **3, 7** and **12** were obtained and peaks were detected which can be assigned to a di-hydrated species. In contrast, for compounds **5**, **10** and **14**, the detected peaks can only tentatively be assigned to the mono-hydrated species (**Figure S15** and **Figure S17**). UV-Vis spectra were monitored over time to confirm the species in aqueous solution. The spectra observed for all $RuCl_2L_2$ compounds show a decrease in A_{max} in the region of 200→320 nm, and predominantly hypsochromic shifts ranging from 11→414 eV (**Table S8**). A decrease in A_{max} is observed in the region of 550→650 nm which could suggest a MLCT, however the spectral peaks are too broad to assign specific hypsochromic shifts and charge transfer bands. Therefore, the changes observed in all UV-Vis spectra at shorter wavelengths have been assigned to intraligand $\pi \rightarrow \pi^*$ transitions.[99] ES-MS analysis was also obtained for the RuI_2L_2 compounds **23**, **26**, **27** and **28**, and the peaks were tentatively assigned to the mono-hydrated species for all four compounds (**Figure S16**) and the UV-Vis spectra also show changes in the MLCT region but are too broad to assign to specific charge transfer bands (**Figure S9**). All compounds show hypochromic nature when monitored in aqueous solution over time, which also correlates to a decrease in initial concentration of both the $RuCl_2L_2$ and RuI_2L_2 compounds. The decrease in initial concentration has been plotted against time (**Figure 11**) and shows the largest effects for the RuI_2L_2 compounds, which are the most active against all cell lines tested. UV-Vis data also shows isosbestic points, suggesting the halide compounds are in equilibrium with a possible hydrated species, which is potentially the active compound and therefore hydrolysis may be the key to the high activities observed for the diiodide compounds.

Conclusions

We have presented a library of 31 *bis*-picolinamide ruthenium(III) dihalide complexes, which contain a mixed ligand system where one picolinamide ligand is bound (*N,N*), whilst the other is bound (*N,O*). The $RuCl_2L_2$ and RuI_2L_2 compounds have been prepared to allow pairwise comparison of the effects of dihalide ligand. X-ray crystallographic analysis has been obtained for fifteen of the new compounds, and confirms the binding mode of the picolinamide ligand, and that these complexes are all in the +3 oxidation state. Some of the $RuCl_2L_2$ complexes were found to co-crystallise with different crystal morphologies reflecting their ability to form more than one structural isomer and switch isomeric configuration. The *cis(X)-cis(N,N)-cis(N,O)*, *cis(X)-trans(N,N)-cis(N,O)* and *trans(X)-trans(N,N)-trans(N,O)* arrangements have all been observed. In contrast, only a single stable *trans(X)-trans(N,N)-trans(N,O)*

Figure 11 Time-dependence formation new species in aqueous solution for **(a)**

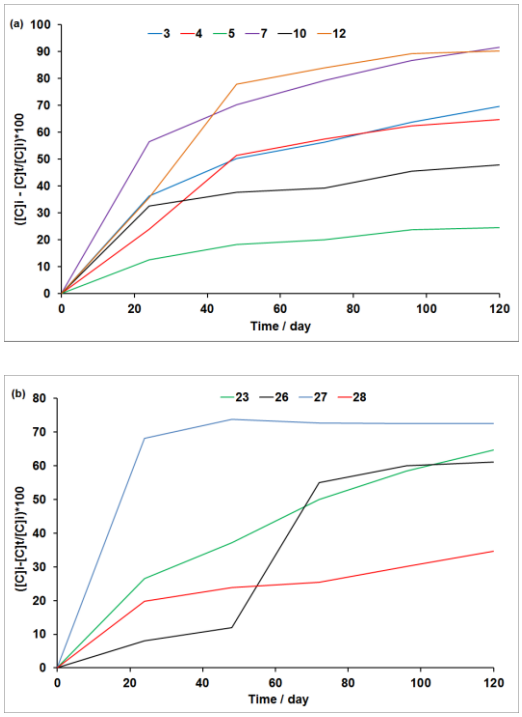

compounds **3**, **5**, **7**, **10**, **12** and **14** in 10% MeOH/90% H_2O and **(b)** compounds **23**, **26**, **27** and **28** in 10% DMF/90% H_2O at 293 K

isomer was obtained for the RuI_2L_2 complexes. This has been confirmed by single crystal X-ray crystallography and powder X-ray diffraction. The ability to synthesise and purify single isomers of the diiodide complexes is very important for the further development of these complexes as potential drugs. Through knowing the configuration of the active drug and being able to synthesise these as single isomers, this eliminates future potential isomer-related formulation issues. The library of complexes was evaluated against several different human cancer cell lines for potential cytotoxic activity. Many of the complexes showed significant cytotoxicity with IC_{50} values commonly in the low μM range. Activity was both ligand- and structure- dependent with several clear structure-activity relationships emerging. As exemplified by cisplatin and transplatin, historically *trans* isomers have generally been found to be less active than their *cis* isomers. Interestingly, this study identifies picolinamide ruthenium (III) diiodide complexes which form a single *trans* isomer, that are significantly more potent than their dichloride analogues which form a mixture of *cis* and *trans* isomers. For both ruthenium dichloride and ruthenium diiodide complexes, enhanced potency was also consistently observed when an electron-withdrawing substituent was placed in the *meta* or *para* position on the picolinamide ligand.

A preliminary evaluation of the selectivity of these picolinamide ruthenium(III) dihalide complexes towards cancer cells versus non-cancer cells was undertaken. The ruthenium diiodide complexes, as well as being more potent (**Table 4**) were also more selective towards cancer cells than their dichloride analogues (**Figure 9**). For both ruthenium diiodide and ruthenium

dichloride complexes, substitution of R = 4'-F/Cl/Br with R = 2',4'-diF/diCl/diBr reduced potency, however, these substitutions increased cancer selectivity (**Figure 10**) indicating the importance of assessing both potency and selectivity in selection of potential lead compounds for further investigation.

The picolinamide ruthenium (III) dihalide complexes were evaluated for activity against the cisplatin-resistant human ovarian cancer cell line A2780cis. Importantly, many of the diiodide complexes showed good activity against the cisplatin-resistant human ovarian cancer cell line A2780cis, with several complexes being more potent against cisplatin-resistant A2780 cancer cells than cisplatin-sensitive A2780 cancer cells. In the development of new organometallic anti-cancer drugs, there is a need for compounds that are not cross resistant with cisplatin and have good selectivity towards cancer cells as opposed to normal cells. These studies have identified a number of highly potent compounds that have good activity against cisplatin resistant A2780 cells and good cancer cell selectivity. Of all the compounds tested, complexes **25** and **30** particularly emerge as good lead candidates for further evaluation based on their potency (**Table 4**), lack of cross resistance in the cisplatin resistant A2780cis cells (**Figure 8**) and good selectivity towards cancer cells compared to normal cells (**Figure 10**). Studies were performed in aqueous solution to gain an understanding of hydrolysis steps in the compounds mode of action. UV-Vis and ES-MS data suggest the possibility of hydrated species in aqueous solution, and the decrease in concentration of the initial compounds is most significant for the RuI_2L_2 compounds. These hydrated species are potentially the active species; however, further studies are required in order isolate these products and understand their effects *in vitro*. Understanding the mode of action of these intermediate species could help to enhance both potency and cancer selectivity by tuning compound design.

Experimental Section

General

All complexes are air stable and the reactions were carried out in air. Chemicals were obtained from Sigma-Aldrich Chemical Co., Acros Organics, Alfa Aesar and Strem Chemical Co., and unless otherwise stated were used as supplied. General preparation and characterisation data by IR, ES+MS, μ_{eff} values and microanalysis for complexes **1** - **31** are reported here. In addition, general preparation and characterisation data for *N*-Ph-picolinamide ligands are also given.

Instrumentation

All NMR spectra were recorded on a Bruker DPX 300 spectrometer, a Bruker DRX 500 spectrometer or a Bruker DRX 500 spectrometer. Elemental analyses were acquired at the University of Leeds Microanalytical Service. Mass Spectra were recorded on a Bruker maXis impact mass spectrometer or on a Micromass ZMD spectrometer with electrospray ionisation and photoiodide array analyser at the University of Leeds Mass Spectrometry Service. Infrared spectra were obtained using a Platinum ATR Spectroscopy on a crystal plate with samples analysed using OPUS software. Magnetic susceptibilities were measured using a Sherwood Scientific Susceptibility at room temperature.

Elemental Analysis

All biologically evaluated compounds must demonstrate a purity >95%, and so the compounds synthesised within this report have been analysed using elemental (CHN) analysis, by a means of combustion. This technique requires the sample to be burned in an excess of oxygen and has a variety of traps which collect the combustion products: CO_2, H_2O and N_2. These masses are then used to help calculated the masses of the 'unknown' product. The experimental values are compared with the calculated values of the sample, and all synthesised compounds herein are within 0.5% of the calculated values.

X-ray crystallographic analysis

A suitable single crystal was selected and immersed in an inert oil. The crystal was then mounted on a glass capillary and attached to a goniometer head on a Bruker X8 Apex diffractometer using graphite monochromated Mo-K_α radiation (λ = 0.71073 Å) or Agilent SuperNova X-ray diffractometer fitted with an Atlas area detector and a kappa-geometry 4-circle goniometer, using graphite monochromated Mo-K_α radiation (λ = 0.71073 Å) or Cu -K_α, (λ = 1.5418 Å), using 1.0° φ-rotation frames. The crystal was cooled to 100-150 K by an Oxford Cryostream low temperature device.[100] The full data set was recorded and the images processed using APEX2[101] or CrysAlis Pro software.[102] Structure solution by direct method was achieved through the use of SHELXS programs,[103] and the structural model defined by full matrix least squares on F^2 using SHELX97[104] and SHELXS 2014/7.[105] Molecular graphics were plotted using Mercury.[106] Editing of CIFs and construction of tables and bond lengths and angles was achieved using WC[107] and PLATON,[108] or Olex2 program.[109] Unless otherwise stated, hydrogen atoms were placed using idealised geometric positions (with free rotation for methyl groups), allowed to move in a "riding model" along with the atoms to which they are attached, and refined isotropically. SQUEEZE[110] routine was used to remove disordered solvent molecules present in complex **7** and **12**.

Cell Line Chemosensitivity Studies

In vitro chemosensitivity tests were performed by the MTT assay against A2780 (human ovarian adenocarcinoma), A2780cis (human ovarian cisplatin resistant adenocarcinoma), HT-29 (human colon adenocarcinoma) and ARPE-19 non-cancer cell lines. Cells were incubated in 96-well plates at a concentration of 2×10^3 cells /well for 24 hours at 37 °C in an atmosphere of 5% CO_2 prior to drug exposure. Complexes **1-31** were all dissolved in dimethylsulfoxide and diluted further with medium to obtain drug solutions ranging from 250 to 0.49 µM. The final dimethylsulfoxide concentration was 0.1% (v/v) which is non-toxic to cells. Drug solutions or DMSO solvent control were applied to cells and incubated for 5 days at 37 °C in an atmosphere of 5% CO_2. For short drug exposure times, after 1, 3 or 6 h media containing the drug was removed and the cells washed twice with PBS before addition of fresh complete media for a further 5 days. Cell survival was determined using the MTT assay as described.[48] On day 5, MTT (20 µL of a 5 mg/mL stock) was added to each well and plates were incubated for a further 3 hours at 37 °C in an atmosphere of 5% CO_2. The solutions were then removed and 150 µL of dimethylsulfoxide was added to each well to dissolve the purple formazan crystals. A Thermo Scientific Multiskan EX microplate spectrophotometer was used to measure the absorbance at 540 nm. Lanes containing medium only and cells in medium (no drug, solvent control) were used as blanks for the spectrophotometer and 100% cell survival respectively. Cell survival was determined as the absorbance of treated cells divided by the absorbance of controls and expressed as a percentage. The IC_{50} values were determined from plots of % survival against drug concentration. Each experiment was repeated 3 times and a mean value obtained.

Chemosensitivity Under Hypoxic Conditions

The hypoxia assay was conducted according to the protocol stated previously for normoxic conditions. However, during the incubation period, the addition of the drug dilutions and the addition of the MTT solution were carried out inside a Don Whitley Scientific H35 Hypoxystation which was set at 0.1% O_2. Drug solutions of complexes and tirapazimine (TPZ) were incubated for 5 days and cell survival was determined using the MTT assay as described.

Hydrolysis Studies

Samples were prepared by dissolving complexes **3**, **5**, **7**, **10**, **12** and **14** in 10% methanol, and complexes **23**, **26**, **27** and **28** in 10% DMF, followed by the addition of 90% deionised water to give a final concentration of 70 µM. These aqueous solutions were scanned at various time points by UV-Vis Spectrophotometry over 5 days at 293 K. The concentration of the complex was determined from a calibration curve or each complex taken at a specific wavelength of maximum absorbance to calculate the percentage of hydrolysed complex.

Data Analysis

Statistical analysis of the results was conducted using Student's *t*-test. For *p*-values < 0.05 are considered as significant, and *p* values < 0.01 as very significant.

***N*-Ph-picolinamide Ligand Preparation**

The ligands used for complexes **1**-**10** and **16**-**26** have been previously reported,[19b] and were prepared using the same synthetic route, which is a modification of the published procedure by Bhattacharya *et al*.[19b] The yields varied in the range 37-69%. The general procedure of and characterisation data of new ligands **L11**-**15** (used for complexes **11**-**15** and **27**-**31**) are also provided.

Functionalised aniline (25 mmol) was added to a solution of pyridine-2-carboxylic acid (25 mmol) in pyridine (15 ml) and warmed to 50°C for 15 minutes. To this mixture, triphenylphosphite (25 mmol) was added and heated to 110°C for 18 hours yielding an orange solution. Addition of water (100 ml) yielded a white paste, to which dichloromethane (40 ml) was added and the organic layer separated from the aqueous layer. The product in the aqueous layer was extracted with 1:1 (v/v) aqueous HCl (3 x 100 ml). To neutralise the extract, sodium bicarbonate was added until pH 7. The brown solid was isolated by filtration then washed with distilled water. After recrystallisation of the product from methanol, washing with water and drying *in vacuo*, yields pale brown needle-like crystals.

Ligand 11: Yield: 3.48 g, 12.6 mmol, 50%. **ES+MS** ($CHCl_3$, m/z): 298.98 [M Na]$^+$. **Anal. Found:** C 52.0%, H 3.2%, N 10.3%, Br 28.9%. **Anal. Calc.:** C 52.0%, H 3.3%, N 10.1%, Br 28.8%. **^{1}H NMR** ($CDCl_3$, 300.13 MHz, 300K) δ 10.72 (br. s, 1H, CON*H*), 8.70 (d, 1H, ^3J(^{1}H-^{1}H) = 4.7 Hz, CH of C_5H_4N), 8.60 (dd, 1H, ^3J(^{1}H-^{1}H) = 8.3 Hz, ^4J(^{1}H-^{1}H) = 1.4 Hz CH of C_5H_4N), 8.32 (d, 1H, ^3J(^{1}H-^{1}H) = 7.8 Hz, CH of C_6H_4Br), 7.94 (td, 1H, ^3J(^{1}H-^{1}H) = 7.7 Hz, ^4J(^{1}H-^{1}H) = 1.7, CH of C_5H_4N), 7.62 (dd, 1H, ^3J(^{1}H-^{1}H) = 8.0 Hz, ^4J(^{1}H-^{1}H) = 1.3 Hz, CH of C_6H_4Br), 7.53 (ddd, 1H, ^3J(^{1}H-^{1}H) = 7.5 Hz, ^4J(^{1}H-^{1}H) = 4.8 Hz, ^5J(^{1}H-^{1}H) = 1.6 Hz, CH of C_5H_4N), 7.40 (m, 1H, CH of C_6H_4Br), 7.04 (td, 1H, ^3J(^{1}H-^{1}H) = 7.7 Hz, ^4J(^{1}H-^{1}H) = 1.5 Hz, CH of C_6H_4Br). **^{13}C{^{1}H} NMR** ($CDCl_3$, 75.47 MHz, 300 K) δ 162.28 (Q, *C*ONH), 149.78 (Q), 148.33 (CH of C_5H_4N), 137.64 (CH of C_5H_4N), 135.94 (Q), 132.49 (CH of C_5H_4N), 128.37 (CH of C_6H_4Br), 126.62 (CH of C_6H_4Br), 125.13 (CH of C_6H_4Br), 122.43 (CH of C_6H_4Br), 121.41 (CH of C_5H_4N), 113.90 (Q, CBr of C_6H_4Br). **IR** (cm^{-1}): 3288 (m), 3105 (m), 1691 (s), 1577 (m), 1503 (m), 1462 (w), 1429 (w), 1375 (s), 1294 (s), 1227 (w), 1146 (w), 1119 (m), 1072 (s), 1038 (s), 997 (s), 890 (m), 857 (m), 822 (s), 748 (s), 682 (s), 621 (m), 540 (s)

Ligand 12: Yield: 3.90 g, 14.1 mmol, 56%. **ES+MS** ($CHCl_3$, m/z): 298.98 [M Na]$^+$). **Anal.Calc.:** C 52.0%, H 3.3%, N 10.1%, Br 28.8%. **Anal. Found:** C 52.1%, H 3.2%, N 10.3%, Br 28.5%. **^{1}H NMR** ($CDCl_3$, 300.13 MHz, 300K) δ 10.06 (br. s, 1H, NH), 8.61 (d, 1H, ^3J(^{1}H-^{1}H) = 3.6 Hz, CH of C_5H_4N), 8.29 (d, 1H, ^3J(^{1}H-^{1}H) = 7.8 Hz, CH of C_5H_4N), 8.05 (s, 1H, CH of C_6H_4Br), 7.92 (t, 1H, ^3J(^{1}H-^{1}H) = 7.6 Hz, CH of C_5H_4N), 7.69 (d, 1H, ^3J(^{1}H-^{1}H) = 7.7 Hz, CH of C_6H_4Br), 7.5 (dd, 1H, ^3J(^{1}H-^{1}H) = 7.0 Hz, ^4J(^{1}H-^{1}H) = 4.8 Hz, CH of C_5H_4N), 7.25 (m, 2H, CH of C_6H_4Br). **^{13}C{^{1}H} NMR** ($CDCl_3$, 75.47 MHz, 300 K) δ 161.96 (Q, *C*ONH), 149.37 (Q), 147.93 (CH of C_5H_4N), 139.04 (Q), 137.88 (CH of C_5H_4N), 130.36 (CH of C_6H_4Br), 127.30 (CH of C_6H_4Br), 126.70 (CH of C_5H_4N), 122.76 (Q, CBr of C_6H_4Br), 122.61 (CH of C_5H_4N), 118.15 (CH of C_6H_4Br). **IR** (cm^{-1}): 3335 (s), 3058 (m), 1698 (s), 1590 (m), 1537 (m), 1483 (m), 1402 (m), 1314 (s), 1234 (s), 1160 (w), 1125 (m), 1092 (m), 1038 (m), 997 (s), 897 (m), 850 (s), 810 (m), 769 (s), 661 (s), 587 (s)

Ligand 13: Yield: 4.78 g, 17.2 mmol, 69%. **ES+MS** ($CHCl_3$, m/z): 298.98 [M Na]$^+$). **Anal. Found:** C 51.8%, H 3.2%, N 10.4%, Br 28.9%. **Anal. Calc.:** C 52.0%, H 3.3%, N 10.1%, Br 28.8%. **^{1}H NMR** ($CDCl_3$, 300.13 MHz, 300K) δ 10.06 (br. s, 1H, NH), 8.63 (d, 1H, ^3J(^{1}H-^{1}H) = 4.7 Hz, CH of C_5H_4N), 8.31 (d, 1H, ^3J(^{1}H-^{1}H) = 7.8 Hz, CH of C_5H_4N), 7.94 (td, 1H, ^3J(^{1}H-^{1}H) = 7.7 Hz, ^4J(^{1}H-^{1}H) = 1.7 Hz, CH of C_5H_4N), 7.71 (d, 2H, ^3J(^{1}H-^{1}H) = 8.8 Hz, CH of C_6H_4Br), 7.52 (m, 3H, CH of C_5H_4N & 2 x CH of C_6H_4Br). **^{13}C{^{1}H} NMR** ($CDCl_3$, 75.47 MHz, 300 K) δ 161.99 (Q, *C*ONH), 149.51 (Q), 147.98 (CH of C_5H_4N), 137.79 (CH of C_5H_4N), 136.85 (Q), 132.06 (CH of C_6H_4Br), 126.63 (CH of C_5H_4N), 122.47 (CH of C_5H_4N), 121.21 (CH of C_6H_4Br), 116.87 (Q, CBr of C_6H_4Br). **IR** (cm^{-1}): 3335 (s), 3058 (m), 1691 (w), 1590 (w), 1490 (w), 1227 (m), 1186 (w), 1099 (w), 1038 (w), 997 (m), 816 (m), 688 (m), 614 (s), 506 (s), 486 (m)

Ligand 14: Yield: 3.83 g, 10.8 mmol, 43%. **ES+MS** ($CHCl_3$, m/z): 378.9 [M Na]$^+$). **Anal. Found:** C 40.6%, H 2.2%, N 7.7%, Br 44.7%.**Anal. Calc.:** C 40.5%, H 2.3%, N 7.9%, Br 44.9%. **^{1}H NMR** ($CDCl_3$, 300.13 MHz, 300K) δ 10.63 (br. s, 1H, NH), 8.60 (d, 1H, ^3J(^{1}H-^{1}H) = 4.7 Hz, CH of C_5H_4N), 8.50 (d, 1H, ^3J(^{1}H-^{1}H) = 8.9 Hz, CH of C_5H_4N), 8.22 (d, 1H, ^3J(^{1}H-^{1}H) = 7.8 Hz, CH of $C_6H_3Br_2$), 7.86 (td, 1H, ^3J(^{1}H-^{1}H) = 7.7 Hz, ^4J(^{1}H-^{1}H) = 1.7, CH of C_5H_4N), 7.68 (d, 1H, ^3J(^{1}H-^{1}H) = 2.3 Hz, CH of $C_6H_3Br_2$), 7.44 (m, CH of C_5H_4N & CH of $C_6H_3Br_2$). **^{13}C{^{1}H} NMR** ($CDCl_3$, 75.47 MHz, 300 K) δ 162.31 (Q, *C*ONH), 149.50 (Q), 148.39 (CH of C_5H_4N), 137.76 (CH of C_5H_4N), 135.24 (Q), 134.68 (CH of $C_6H_3Br_2$), 131.43 (CH of $C_6H_3Br_2$), 126.83 (CH of C_5H_4N), 122.56 (CH of $C_6H_3Br_2$), 122.27 (CH of C_5H_4N), 116.65 (Q, CBr of $C_6H_3Br_2$), 114.28 (Q, CBr of $C_6H_3Br_2$). **IR** (cm^{-1}): 3288 (m), 3112 (m), 1691 (s), 1563 (m), 1509 (m), 1456 (w), 1381 (m), 1301 (s), 1234 (w), 1113 (m), 1078 (m), 1038 (s), 997 (m), 890 (m), 863 (m), 810 (s), 742 (m), 669 (s), 621 (m), 540 (m)

Ligand 15: Yield: 3.26 g, 9.17 mmol, 37%. **ES+MS** ($CHCl_3$, m/z): 356.90 [M H]$^+$. **Anal. Found:** C 40.6%, H 2.3%, N 7.7%, Br 44.8%. **Anal. Calc.:** C 40.5%, H 2.3%, N 7.9%, Br 44.9%. **^{1}H NMR** ($CDCl_3$, 300.13 MHz, 300K) δ 10.65 (br. s, 1H, NH), 8.82 (d, 1H, ^3J(^{1}H-^{1}H) = 2.4 Hz), 8.61 (d, 1H, ^3J(^{1}H-^{1}H) = 4.7 Hz, CH of C_5H_4N), 8.22 (d, 1H, ^3J(^{1}H-^{1}H) = 7.8 Hz, CH of C_5H_4N), 7.86 (td, 1H, ^3J(^{1}H-^{1}H) = 7.7 Hz, ^4J(^{1}H-^{1}H) = 1.7, CH of C_5H_4N), 7.45 (ddd, 1H, ^3J(^{1}H-^{1}H) = 7.6 Hz, ^4J(^{1}H-^{1}H) = 4.7 Hz, ^5J(^{1}H-^{1}H) = 1.2 Hz, CH of C_5H_4N), 7.38 (d, 1H, ^3J(^{1}H-^{1}H) = 8.6 Hz, H_e), 7.08 (dd, 1H, ^3J(^{1}H-^{1}H) = 8.5 Hz, ^4J(^{1}H-^{1}H) = 2.4 Hz). **^{13}C{^{1}H} NMR** ($CDCl_3$, 75.47 MHz, 300 K) δ 162.31 (Q, *C*ONH), 149.38 (Q), 148.38 (CH of C_5H_4N), 137.76 (CH of C_5H_4N), 137.05 (Q), 133.36 (CH of $C_6H_3Br_2$), 128.00 (CH of $C_6H_3Br_2$), 126.87 (CH of C_5H_4N), 124.01 (CH of $C_6H_3Br_2$), 122.58 (CH of C_5H_4N), 121.25 (Q, CBr of $C_6H_3Br_2$), 112.21 (Q, CBr of $C_6H_3Br_2$). **IR** (cm^{-1}): 3301 (s), 3112 (s), 1698 (m), 1570 (m), 1516 (m), 1288 (m), 1227 (m), 1112 (m), 1018 (s), 870 (s), 803 (s), 742 (s), 675 (s), 580 (m), 500 (m)

Preparation of Complexes 1-**16**

Functionalised *N*-phenyl picolinamide (0.80 mmol) was added to a solution of $RuCl_3.3H_2O$ (0.40 mmol) in ethanol (30 mL), followed by addition of triethylamine (0.40 mmol). The solution was heated under reflux for 2 hours giving a red-orange solution. The volume of solvent was reduced by one third to yield an orange solid. The solid was filtered, washed with pentane, dried *in vacuo* and recrystallised *via* vapor diffusion in methanol-pentane yielding red crystals.

Complex 1: Yield: 0.347 g, 0.60 mmol, 74%. μ_{eff} = 1.97 ± 0.12 μ_B. **ES+MS** (CH_3OH, m/z): 568.0 [M H]$^+$. **Anal. Found:** C 46.9; H 3.60; N 8.9 %. **Anal. Calc.:** C 46.4; H 4.0; N 9.0%. **IR** (cm^{-1}): 3482 (b), 3260 (w), 3200 (m), 3058 (s), 1617 (b), 1570 (s), 1490 (b), 1449 (b), 1355 (s), 1294 (s), 1146 (s), 1025 (s), 997 (w), 971 (s), 897 (s), 836 (w), 803 (s), 748 (s), 688 (s), 587 (s), 506 (s)

Complex 2: Yield: 0.12 g, 0.20 mmol, 50%. μ_{eff} = 1.97 ± 0.12 μ_B. **ES+MS** (CH_3OH, m/z): 604.0 [M H]$^+$. **Anal. Found:** C 45.1; H 3.3; N 8.6%. **Anal. Calc.:** C 45.1; H 3.3; N 8.8%. IR (cm^{-1}): 3489 (b), 3200 (w), 3065 (m), 1617 (b), 1577 (s), 1496 (s), 1449 (w), 1355 (s), 1301 (s), 1267 (s), 1206 (s), 1153 (s), 1099 (s), 1031 (s), 964 (s), 917 (s), 863 (s), 755 (s), 682 (s), 601 (s), 547 (w), 519 (w), 473 (s)

Complex 3: Yield: 0.13 g, 0.21 mmol, 52%. μ_{eff} = 1.83 ± 0.03 μ_B. **ES+MS** (CH_3OH, m/z): 604.0 [M H]$^+$. **Anal. Found:** C 44.4; H 3.1; N 8.4%. **Anal. Calc.:** C 43.9; H 3.5; N 8.5%. **IR** (cm^{-1}): 3510 (b), 3254 (w), 3220 (w), 3058 (m), 1624 (b), 1469 (w), 1409 (s), 1348 (s), 1294 (w), 1234 (s), 1153 (s), 1092 (w), 1058 (w), 1018 (w), 971 (w), 904 (s), 829 (s), 762 (w), 688 (s), 547 (w), 507 (w), 493 (w)

Complex 4: Yield: 0.18 g, 0.28 mmol, 72%. μ_{eff} = 1.87 ± 0.07 μ_B. **ES+MS** (CH_3OH, m/z): 640.0 [M H]$^+$. **Anal. Found:** C 43.1; H 2.8; N 8.0%. **Anal. Calc.:** C 42.7; H 2.8; N 8.3%. **IR** (cm^{-1}): 3470 (b), 3220 (w), 3058 (m), 1611 (b), 1503 (w), 1469 (w), 1429 (w), 1355 (s), 1301 (w), 1260 (w), 1220 (m), 1139 (s), 1092 (s), 1052 (m), 1031 (m), 964 (s), 924 (m), 850 (m), 803 (m), 755 (m), 735 (w), 694 (s), 607 (m), 540 (m), 459 (m)

Complex 5: Yield: 0.07 g, 0.11 mmol, 28%. μ_{eff} = 1.96 ± 0.16 μ_B. **ES+MS** (CH_3OH, m/z): 641.96 [M]$^+$. **Anal. Found:** C 43.1; H 3.1; N 8.2%. **Anal. Calc.:** C 42.7; H 2.8; N 8.3%. IR (cm^{-1}): 3482 (b), 3207 (w), 3065 (m), 1584 (b), 1496 (w), 1341 (m), 1241 (m), 1206 (w), 1173 (s), 1099 (s), 1058 (w), 978 (s), 924 (w), 870 (m), 762 (s), 688 (s), 587 (w), 506 (w), 473 (s).

Complex 6: Yield: 0.15 g, 0.23 mmol, 58%. μ_{eff} = 2.21 ± 0.07 μ_B. **ES+MS** (CH_3OH, m/z): 637.9 [M H]$^+$. **Anal. Found:** C 43.4; H 3.1; N 8.1; Cl 22.1%. **Anal. Calc.:** C 43.5; H 3.0; N 8.5; Cl 21.4%. **IR** (cm^{-1}): 3476 (b), 3220 (w), 3065 (w), 2856 (w), 1590 (b), 1469 (w), 1442 (w), 1341 (m), 1301 (w), 1260 (w), 1146 (s), 1052 (s), 1031 (m), 964 (m), 924 (s), 850 (w), 803 (m), 755 (s), 688 (s), 601 (m), 500 (m), 452 (w)

Complex 7: Yield: 0.15 g, 0.23 mmol, 55%. μ_{eff} = 2.40 ± 0.04 μ_B. **ES+MS** (CH_3OH, m/z): 637.9 [M H]$^+$. **Anal. Found:** C 44.0; H 3.2; N 8.3; Cl 21.5%. **Anal. Calc.:** C 44.1; H 2.9; N 8.6; Cl 21.7%. **IR** (cm^{-1}): 3442 (b), 3254 (w), 3193 (w), 3065 (m), 1597 (b), 1476 (m), 1435 (w), 1391 (s), 1307 (m), 1260 (m), 1146 (m), 1065 (w), 965 (m), 883 (m), 762 (s), 675 (s), 594 (w), 513 (w)

Complex 8: Yield: 0.07 g, 0.11 mmol, 28%. μ_{eff} = 2.08 ± 0.03 μ_B. **ES+MS** (CH_3OH, m/z): 637.9 [M H]$^+$. **Anal. Found:** C 43.2; H 3.0; N 8.1, Cl 21.8%. **Anal. Calc.:** C 43.5; H 3.0; N 8.5; Cl 21.47%. **IR** (cm^{-1}): 3496 (b), 3247 (w), 3058 (m), 1584 (b), 1490 (m), 1409 (m), 1355 (m), 1294 (m), 1260 (w), 1241 (w), 1146 (m), 1085 (s), 1052 (w), 1018 (s), 971 (m), 910 (m), 822 (s), 755 (s), 722 (m), 688 (s), 506 (s), 466 (w)

Complex 9: Yield: 0.12 g, 0.17 mmol, 44%. μ_{eff} = 1.99 ± 0.06 μ_B. **ES+MS** (CH_3OH, m/z): 705.8 [M H]$^+$. **Anal. Found:** C 39.7; H 2.5; N 7.6, Cl 29.5%. **Anal. Calc.:** C 39.9; H 2.4; N 7.8; Cl 29.4%. **IR** (cm^{-1}): 3510 (b), 3207 (w), 3058 (m), 1590 (b), 1469 (m), 1341 (m), 1301 (w), 1260 (w), 1146 (m), 1099 (s), 1052 (s), 1025 (w), 964 (w), 917 (m), 857 (m), 803 (m), 762 (s), 688 (m), 560 (w), 526 (m)

Complex 10: Yield: 0.11 g, 0.16 mmol, 40%. μ_{eff} = 2.53 ± 0.02 μ_B. **ES+MS** (CH_3OH, m/z): 705.8 [M H]$^+$. **Anal. Found:** C 40.6; H 2.9; N 7.5, Cl 30.0%. **Anal. Calc.:** C 40.9; H 2.2; N 7.9; Cl 30.2%. **IR** (cm^{-1}): 3496 (b), 3200 (w), 3065 (w), 1577 (b), 1469 (m), 1388 (m), 1334 (m), 1301 (w), 1260 (w), 1139 (m), 1092 (m), 1052 (m), 964 (m), 931 (m), 890 (w), 863 (w), 803 (s), 762 (s), 688 (s), 594 (m), 566 (m), 519 (w), 459 (w)

Complex 11: Yield: 0.13 g, 0.18 mmol, 46%. μ_{eff} = 2.02 ± 0.06 μ_B. **ES+MS** (CH_3OH, m/z): 725.8 [M H]$^+$. **Anal. Found:** C 37.6; H 2.6; N 7.1%. **Anal. Calc.:** C 37.9; H 2.8; N 7.4%. **IR** (cm^{-1}): 3496 (b), 3214 (m), 3065 (m), 1584 (s), 1476 (s), 1442 (w), 1348 (s), 1307 (s), 1260 (m), 1146 (m), 1052 (s), 971 (w), 924 (s), 843 (w), 810 (m), 748 (s), 688 (m), 594 (w), 533 (w), 493 (w)

Complex 12: Yield: 0.19 g, 0.25 mmol, 62%. μ_{eff} = 2.05 ± 0.10 μ_B. **ES+MS** (CH_3OH, m/z): 725.8 [M H]$^+$. **Anal. Found:** C 38.8; H 2.6; N 7.3%. **Anal. Calc.:** C 38.8; H 2.6; N 7.5%. **IR** (cm^{-1}): 3489 (b), 3254 (w), 3072 (m), 1570 (b), 1476 (s), 1429 (w), 1348 (s), 1294 (m), 1260 (m), 1146 (m), 1065 (w), 997 (w), 971 (m), 857 (m), 762 (s), 722 (w), 675 (s), 601 (w), 560 (w), 500 (w)

Complex 13: Yield: 0.13 g, 0.17 mmol, 44%. μ_{eff} = 2.04 ± 0.16 μ_B. **ES+MS** (CH_3OH, m/z): 725.8 [M H]$^+$. **Anal. Found:** C 38.9; H 2.8; N 7.4%. **Anal. Calc.:** C 38.8; H 2.6; N 7.5%. **IR** (cm^{-1}): 3482 (b), 3247 (w), 3072 (m), 1570 (b), 1490 (m), 1402 (w), 1348 (m), 1288 (m), 1260 (w), 1146 (m), 1065 (m), 1025 (w), 1004 (s), 964 (w), 910 (w), 822 (s) 755 (s), 688 (s), 513 (s)

Complex 14: Yield: 0.19 g, 0.21 mmol, 51%. μ_{eff} = 2.10 ± 0.14 μ_B. **ES+MS (**CH_3OH, m/z): 882.6 [M]. **Anal. Found:** C 31.8; H 2.1; N 5.9%. **Anal. Calc.:** C 32.0; H 1.9; N 6.2%. **IR** (cm^{-1}): 3496 (b), 3200 (w), 3065 (m), 1584 (b), 1462 (m), 1341 (m), 1301 (m), 1260 (m), 1146 (s), 1072 (s), 1045 (s), 964 (w), 917 (s), 850 (w), 816 (w), 748 (m), 682 (m), 547 (w), 506 (m)

Complex 15: Yield: 0.19 g, 0.21 mmol, 54%. μ_{eff} = 2.03 ± 0.02 μ_B. **ES+MS** (CH_3OH, m/z): 882.6 [M]. **Anal. Found:** C 31.8; H 2.2; N 5.9%. **Anal. Calc.:** C 32.0; H 1.9; N 6.2%. **IR** (cm^{-1}): 3510 (b), 3186 (w), 3065 (m), 1584 (b), 1469 (m), 1388 (m), 1334 (m), 1301 (w), 1267 (w), 1146 (s), 1085 (s), 1031 (s), 971 (m), 931 (m), 870 (m), 810 (m), 755 (s), 694 (s), 601 (w), 566 (w), 506 (m)

Complex 16: Yield: 0.09 g, 0.13 mmol, 34%. μ_{eff} = 2.01 ± 0.01 μ_B. **ES+MS** (CH_3OH, m/z): 819.79 [M]. **Anal. Found:** C 33.3; H 2.2; N 6.2%. **Anal. Calc.:** C 33.7; H 2.5; N 6.6%. **IR** (cm^{-1}): 3476 (b), 3200 (w), 3051 (m), 1590 (s), 1556 (s), 1469 (s), 1435 (w), 1341 (m), 1301 (m), 1146 (m), 1018 (m), 917 (m), 803 (w), 748 (s), 722 (w), 682 (m), 647 (m), 594 (m), 526 (w), 500(m)

Preparation of Complexes 17-31

Functionalised *N*-phenyl picolinamide (0.80 mmol) was added to a solution of $RuCl_3.3H_2O$ (0.40 mmol) in ethanol (30 mL), followed by addition of triethylamine (0.40 mmol). The solution was heated under reflux for 2 hours giving a red-orange solution. An excess of KI (4 mmol) was added and the solution heated under reflux for 18 hours resulting in a dark coloured solution. The solid was filtered, washed with water to remove KCl, dried *in vacuo* and recrystallised *via* vapour diffusion in DMF-ether yielding black/green crystals.

Complex 17: Yield: 0.26 g, 0.35 mmol, 58%. μ_{eff} = 1.68 ± 0.07 μ_B. **ES+MS** (DMF, m/z): 751.9 [M H$^+$]. **Anal. Found:** C 38.8; H 2.7; N 7.3%. **Anal. Calc.:** C 38.4; H 2.6; N 7.5%. **IR** (cm^{-1}): 3288 (b), 3072 (w), 2856 (w), 1570 (s), 1483 (m), 1449 (m), 1368 (w), 1294 (w), 1260 (w), 1173 (w), 1153 (w), 1072 (w), 1025 (w), 903 (w), 755 (s), 694 (s), 587 (m), 513 (m), 473 (w)

Complex 18: Yield: 0.22 g, 0.27 mmol, 59%. μ_{eff} = 1.71 ± 0.07 μ_B. **ES+MS** (DMF, m/z): 787.9 [M H$^+$]. **Anal. Found:** C 35.2; H 2.2; N 6.6%. **Anal. Calc.:** C 35.1; H 2.6; N 6.8%. **IR** (cm^{-1}): 3247 (w), 3072 (w), 2883 (b), 1577 (s), 1490 (m), 1456 (w), 1362 (m), 1301 (w), 1260 (m), 1213 (w), 1153 (w), 1099 (w), 1025 (w), 964 (w), 910 (w), 863 (w), 789 (m), 748 (s), 688 (w), 513 (w), 473 (w)

Complex 19: Yield: 0.24 g, 0.31 mmol, 58%. μ_{eff} = 1.70 ± 0.09 μ_B. ES+MS (DMF, m/z): 787.8 [M H$^+$]. **Anal. Found:** C 37.0; H 2.2; N 7.0%. **Anal. Calc.:** C 36.7; H 2.2; N 7.1%. **IR** (cm^{-1}): 3226 (w), 3072 (w), 2863 (b), 1584 (m), 1496 (m), 1416 (s), 1375 (w), 1348 (w), 1213 (m), 1153 (m), 1085 (w),

1011 (w), 971 (w), 910 (w), 836 (m), 762 (m), 675 (m), 540 (m), 500 (w), 473 (w)

Complex 20: Yield: 0.17 g, 0.20 mmol, 36%. μ_{eff} = 1.83 ± 0.05 μ_B. **ES+MS** (DMF, m/z): 823.8 [M H^+]. **Anal. Found:** C 35.1; H 1.8; N 6.6%. **Anal. Calc.:** C 35.1; H 1.8; N 6.8%. **IR** (cm^{-1}): 3226 (w), 3072 (b), 2883 (w), 1584 (b), 1503 (m), 1429 (w), 1368 (m), 1253 (m), 1213 (w), 1139 (s), 1092 (s), 1018 (w), 957 (s), 910 (m), 863 (m), 803 (m), 762 (s), 675 (s), 601 (s), 573 (w), 533 (s), 473 (m)

Complex 21: Yield: 0.19 g, 0.24 mmol, 31%. μ_{eff} = 1.79 ± 0.04 μ_B. **ES+MS** (DMF, m/z): 823.8 [M H^+]. **Anal. Found:** C 35.0; H 1.8; N 6.8%. **Anal. Calc.:** C 35.2; H 1.8; N 6.8%. **IR** (cm^{-1}): 3214 (w), 3072 (b), 2883 (w), 1577 (b), 1496 (m), 1355 (m), 1247 (m), 1186 (m), 1132 (m), 1085 (m), 1058 (w), 971 (s), 917 (m), 876 (m), 803 (m), 762 (s), 694 (m), 668 (m), 594 (m), 506 (m), 466 (m)

Complex 22: Yield: 0.29 g, 0.36 mmol, 34%. μ_{eff} = 1.77 ± 0.03 μ_B. ES+MS (DMF, m/z): 819.8 [M]. **Anal. Found:** C 36.1; H 2.2; N 6.1%. **Anal. Calc.:** C 36.1; H 2.7; N 6.5%. IR (cm^{-1}): 3226 (w), 3072 (b), 2951 (w), 1563 (s), 1476 (m), 1442 (w), 1355 (m), 1301 (w), 1253 (m), 1153 (w), 1052 (w), 1031 (w), 964 (w), 917 (w), 748 (s), 688 (m), 634 (w), 533 (w), 500 (w)

Complex 23: Yield: 0.21 g, 0.25 mmol, 62%. μ_{eff} = 1.60 ± 0.09 μ_B. **ES+MS** (DMF, m/z): 841.8 [M Na^+]. **Anal. Found:** C 34.6; H 2.2; N 6.7%. **Analy. Calc.:** C 34.4; H 2.3; N 6.7%. **IR** (cm^{-1}): 3240 (w), 3065 (b), 2863 (w), 1563 (s), 1469 (m), 1341 (m), 1301 (w), 1253 (m), 1153 (w), 1072 (w), 991 (w), 937 (w), 883 (m), 789 (m), 762 (s), 668 (m), 587 (w), 566 (w), 513 (w), 473 (w)

Complex 24: Yield: 0.25 g, 0.30 mmol, 60%. μ_{eff} = 1.77 ± 0.02 μ_B. **ES+MS** (DMF, m/z): 819.8 [M]. **Anal. Found:** C 36.4; H 2.3; N 6.7%. **Anal. Calc.:** C 36.1; H 2.7; N 6.5%. **IR** (cm^{-1}): 3254 (w), 3058 (b), 2964 (w), 1556 (s), 1490 (m), 1355 (w), 1267 (w), 1132 (m), 1085 (m), 1011 (m), 971 (w), 910 (w), 822 (m), 762 (s), 722 (w), 688 (w), 513 (s), 473 (w)

Complex 25: Yield: 0.22 g, 0.25 mmol, 44%. μ_{eff} = 1.67 ± 0.08 μ_B. **ES+MS** (DMF, m/z): 889.7 [M H^+]. **Anal. Found:** C 32.8; H 1.7; N 6.2%. **Anal. Calc.:** C 32.5; H 1.7; N 6.3%. **IR** (cm^{-1}): 3240 (w), 3065 (w), 2930 (w), 1550 (m), 1462 (m), 1355 (m), 1267 (w), 1146 (w), 1099 (w), 1058 (w), 964 (w), 910 (w), 857 (s), 803 (w), 762 (s), 682 (m), 560 (m), 506 (m)

Complex 26: Yield: 0.32 g, 0.36 mmol, 44%. μ_{eff} = 1.76 ± 0.14 μ_B. **ES+MS** (DMF, m/z): 887.7 [M]. **Anal. Found:** C 33.6; H 1.8; N 6.3%. **Anal. Calc.:** C 33.4; H 2.3; N 6.0%. **IR** (cm^{-1}): 3207 (w), 3079 (w), 2998 (w), 1537 (b), 1469 (w), 1395 (w), 1355 (w), 1307 (m), 1260 (w), 1152 (s), 1092 (s), 1052 (s), 1025 (w), 971 (s), 931 (s), 897 (w), 876 (s), 803 (s), 755 (s), 682 (s), 580 (m), 513 (s), 459 (s)

Complex 27: Yield: 0.30 g, 0.33 mmol, 52%. μ_{eff} = 1.65 ± 0.09 μ_B. **ES+MS** (DMF, m/z): 909.7 [M H^+]. **Anal. Found:** C 31.9; H 2.1; N 6.0%. **Anal. Calc.:** C 31.7; H 1.9; N 6.2%. **IR** (cm^{-1}): 3214 (w), 3051 (w), 2876 (w), 1570 (m), 1469 (w), 1341 (w), 1301 (w), 1253 (w), 1139 (m), 1031 (m), 964 (w), 917 (w), 850 (w), 803 (w), 748 (s), 682 (m), 601 (w), 526 (m), 500 (m)

Complex 28: Yield: 0.17 g, 0.19 mmol, 50%. μ_{eff} = 1.81 ± 0.06 μ_B. **ES+MS** (DMF, m/z): 931.7 [M Na^+]. **Anal. Found:** C 31.8; H 1.9; N 6.1%. **Anal. Calc.:** C 31.7; H 1.9; N 6.2%. **IR** (cm^{-1}): 3260 (w), 3065 (w), 2930 (w), 1556 (m), 1462 (w), 1341 (w), 1294 (w), 1247 (w), 1146 (w), 1065 (w), 991 (w), 931 (w), 870 (w), 782 (w), 755 (s), 675 (m), 587 (w), 547 (w), 473 (w)

Complex 29: Yield: 0.27 g, 0.30 mmol, 52%. μ_{eff} = 1.92 ± 0.05 μ_B. **ES+MS** (DMF, m/z): 909.7 [M H^+]. **Anal. Found:** C 31.8; H 1.9; N 5.9%. **Anal. Calc.:** C 31.7; H 1.9; N 6.2%. **IR** (cm^{-1}): 3247 (w), 3065 (w), 2937 (w), 1556 (m), 1476 (w), 1355 (w), 1294 (w), 1260 (w), 1227 (w), 1146 (w), 1065 (w), 1011 (w), 964 (w), 910 (w), 822 (m), 755 (m), 688 (w), 506 (s)-, 473 (w)

Complex 30: Yield: 0.34 g, 0.32 mmol, 74%. μ_{eff} = 1.68 ± 0.05 μ_B. **ES+MS** (DMF, m/z): 1090.5 [M Na^+ H^+]. **Anal. Found:** C 28.0; H 1.5; N 5.2%. **Anal. Calc.:** C 28.1; H 1.9; N 5.0%. **IR** (cm^{-1}): 3233 (w), 3065 (w), 2917 (w), 1550 (m), 1462 (m), 1348 (m), 1260 (w), 1132 (w), 1078 (w), 1038 (m), 964 (w), 917 (w), 843 (m), 802 (m), 755 (m), 688 (m), 547 (w), 526 (w), 500 (w)

Complex 31: Yield: 0.27 g, 0.25 mmol, 33%. μ_{eff} = 1.85 ± 0.10 μ_B. **ES+MS** (DMF, m/z): 1067.5 [M H^+]. **Anal. Found:** C 27.8; H 1.5; N 5.1%. **Anal. Calc.:** C 28.1; H 1.9; N 5.0%. **IR** (cm^{-1}): 3207 (w), 3058 (w), 2917 (w), 1544 (m), 1462 (m), 1388 (m), 1348 (m), 1301 (w), 1146 (m), 1072 (m), 1025 (s), 964 (w), 931 (w), 870 (w), 803 (w), 755 (m), 688 (m), 607 (w), 500 (w)

Acknowledgements

We would like to thank Dr. Marc Little (Leeds) for assistance in solving structure **5**, Mr. Pablo Caramés-Méndez (Leeds) for providing additional NMR data and Mr. Andrew Healey (Bradford) for additional mass spectrometry data. We also thank Mr. Simon Barrett, Mr. Ian Blakely and Ms. Tanya Marinko Covell at the University of Leeds Microanalytical Service for assistance in NMR, mass spectrometry and microanalysis.

Keywords: Anti-cancer • Cytotoxicity • Isomers • Ruthenium(III) • *trans*-compounds

[1] M. J. Cleare, J. D. Hoeschele, *Bioinorg. Chem.* **1973**, *2*, 187–210.
[2] M. Coluccia, A. Nassi, F. Loseto, A. Boccarelli, M. A. Mariggio, D. Giordano, F. P. Intini, P. Caputo, G. Natile, *J. Med. Chem.* **1993**, *36*, 510–512.
[3] D. Wang, S. J. Lippard, *Nat Rev Drug Discov* **2005**, *4*, 307–320.
[4] L. R. Kelland, C. F. J. Barnard, K. J. Mellish, M. Jones, P. M. Goddard, M. Valenti, A. Bryant, B. A. Murrer, K. R. Harrap, *Cancer Res.* **1994**, *54*, 5618.
[5] J. M. Pérez, M. A. Fuertes, C. Alonso, C. Navarro-Ranninger, *Crit Rev Onco Hemol* **2000**, *35*, 109–120.
[6] N. Farrell, T. T. B. Ha, J. P. Souchard, F. L. Wimmer, S. Cros, N. P. Johnson, *J. Med. Chem.* **1989**, *32*, 2240–2241.
[7] M. Coluccia, A. Boccarelli, M. A. Mariggio, P. Cardellicchio, P. Caputo, F. P. Intini, G. Natile, *Chem Biol Int* **1995**, *98*, 251–266.
[8] C. Bartel, A. K. Bytzek, Y. Y. Scaffidi-Domianello, G. Grabmann, M. A. Jakupec, C. G. Hartinger, M. Galanski, B. K. Keppler, *JBIC J. Biol. Inorg. Chem.* **2012**, *17*, 465–474.
[9] N. Farrell, J. A. Woods, L. Salassa, Y. Zhao, K. S. Robinson, G. Clarkson, F. S. Mackay, P. J. Sadler, *Angew Chem Int Ed* **2010**, *49*, 8905–8908.
[10] N. Farrell, L. R. Kelland, J. D. Roberts, M. Van Beusichem, *Cancer Res.* **1992**, *52*, 5065.
[11] J. B. Aitken, S. Antony, C. M. Weekley, B. Lai, L. Spiccia, H. H. Harris, *Metallomics* **2012**, *4*, 1051–1056.
[12] G. Sava, S. Zorzet, C. Turrin, F. Vita, M. Soranzo, G. Zabucchi, M. Cocchietto, A. Bergamo, S. DiGiovine, G. Pezzoni, et al., *Am. Assoc. Cancer Res.* **2003**, *9*, 1898–1905.
[13] B. K. Keppler, W. Rupp, *J. Cancer Res. Clin. Oncol.* **1986**, *111*, 166–168.
[14] A. Bergamo, A. Masi, M. A. Jakupec, B. K. Keppler, G. Sava, *Met.-Based Drugs* **2009**, *2009*, 681270.
[15] B. K. Keppler, W. Rupp, U. M. Juhl, H. Endres, R. Niebl, W. Balzer, *Inorg. Chem.* **1987**, *26*, 4366–4370.
[16] G. Sava, S. Pacor, G. Mestroni, E. Alessio, *Clin. Exp. Metastasis* **1992**, *10*, 273–280.
[17] A. Bergamo, R. Gagliardi, V. Scarcia, A. Furlani, E. Alessio, G. Mestroni, G. Sava, *J. Pharmacol. Exp. Ther.* **1999**, *289*, 559–564.
[18] G. Sava, I. Capozzi, K. Clerici, G. Gagliardi, E. Alessio, G. Mestroni, *Clin. Exp. Metastasis* **1998**, *16*, 371–379.
[19] M. Bacac, A. C. . Hotze, K. van der Schilden, J. G. Haasnoot, S. Pacor, E. Alessio, G. Sava, J. Reedijk, *J. Inorg. Biochem.* **2004**, *98*, 402–412.
[20] J. M. Rademaker-Lakhai, D. van den Bongard, D. Pluim, J. H. Beijnen, J. H. M. Schellens, *Am. Assoc. Cancer Res.* **2004**, *10*, 3717–3727.

[21] C. G. Hartinger, S. Zorbas-Seifried, M. A. Jakupec, B. Kynast, H. Zorbas, B. K. Keppler, *Spec. Issue Contain. Contrib. 12th Int. Conf. Biol. Inorg. Chem. Issue Contain. Contrib. 12th Int. Conf. Biol. Inorg. Chem.* **2006**, *100*, 891–904.

[22] S. Leijen, S. A. Burgers, P. Baas, D. Pluim, M. Tibben, E. van Werkhoven, E. Alessio, G. Sava, J. H. Beijnen, J. H. M. Schellens, *Invest. New Drugs* **2015**, *33*, 201–214.

[23] A. R. Timerbaev, *TrAC Trends Anal. Chem.* **2016**, *80*, 547–554.

[24] M. Brindell, I. Stawoska, J. Supel, A. Skoczowski, G. Stochel, R. van Eldik, *JBIC J. Biol. Inorg. Chem.* **2008**, *13*, 909–918.

[25] M. Bouma, B. Nuijen, M. T. Jansen, G. Sava, A. Bult, J. H. Beijnen, *J. Pharm. Biomed. Anal.* **2002**, *30*, 1287–1296.

[26] M. I. Webb, C. J. Walsby, *Dalton Trans.* **2011**, *40*, 1322–1331.

[27] M. Brindell, D. Piotrowska, A. A. Shoukry, G. Stochel, R. van Eldik, *JBIC J. Biol. Inorg. Chem.* **2007**, *12*, 809–818.

[28] V. Novohradsky, A. Bergamo, M. Cocchietto, J. Zajac, V. Brabec, G. Mestroni, G. Sava, *Dalton Trans.* **2015**, *44*, 1905–1913.

[29] E. Gallori, C. Vettori, E. Alessio, F. G. Vilchez, R. Vilaplana, P. Orioli, A. Casini, L. Messori, *Arch. Biochem. Biophys.* **2000**, *376*, 156–162.

[30] A. Barca, B. Pani, M. Tamaro, E. Russo, *Mutat. Res. Mol. Mech. Mutagen.* **1999**, *423*, 171–181.

[31] C. G. Hartinger, M. A. Jakupec, S. Zorbas-Seifried, M. Groessl, A. Egger, W. Berger, H. Zorbas, P. J. Dyson, B. K. Keppler, *Chem Biodivers* **2008**, *5*, 2140–2155.

[32] F. Kratz, M. Hartmann, B. Keppler, L. Messori, *J. Biol. Chem.* **1994**, *269*, 2581–2588.

[33] M. Pongratz, P. Schluga, M. A. Jakupec, V. B. Arion, C. G. Hartinger, G. Allmaier, B. K. Keppler, *J. Anal. At. Spectrom.* **2004**, *19*, 46–51.

[34] A. Bergamo, C. Gaiddon, J. H. M. Schellens, J. H. Beijnen, G. Sava, *J. Inorg. Biochem.* **2012**, *106*, 90–99.

[35] F. Lentz, A. Drescher, A. Lindauer, M. Henke, R. A. Hilger, C. G. Hartinger, M. E. Scheulen, C. Dittrich, B. K. Keppler, U. Jaehde, et al., *Anticancer. Drugs* **2009**, *20*.

[36] N. R. Dickson, S. F. Jones, H. A. Burris, *J Clin Oncol* **2011**, *29*, (suppl., abstr. 2607).

[37] P. Heffeter, B. Atil, K. Kryeziu, D. Groza, G. Koellensperger, W. Körner, U. Jungwirth, T. Mohr, B. K. Keppler, W. Berger, *Eur. J. Cancer* **2013**, *49*, 3366–3375.

[38] A. Gavriluta, G. E. Büchel, L. Freitag, G. Novitchi, J. B. Tommasino, E. Jeanneau, P.-S. Kuhn, L. González, V. B. Arion, D. Luneau, *Inorg. Chem.* **2013**, *52*, 6260–6272.

[39] G. E. Büchel, A. Gavriluta, M. Novak, S. M. Meier, M. A. Jakupec, O. Cuzan, C. Turta, J.-B. Tommasino, E. Jeanneau, G. Novitchi, et al., *Inorg. Chem.* **2013**, *52*, 6273–6285.

[40] R. A. Krause, K. Krause, *Inorg. Chem.* **1980**, *19*, 2600–2603.

[41] A. H. Velders, H. Kooijman, A. L. Spek, J. G. Haasnoot, D. de Vos, J. Reedijk, *Inorg. Chem.* **2000**, *39*, 2966–2967.

[42] A. H. Velders, K. van der Schilden, A. C. G. Hotze, J. Reedijk, H. Kooijman, A. L. Spek, *Dalton Trans.* **2004**, 448–455.

[43] E. Wachter, A. Zamora, D. K. Heidary, J. Ruiz, E. C. Glazer, *Chem. Commun.* **2016**, *52*, 10121–10124.

[44] A. Habtemariam, M. Melchart, R. Fernández, S. Parsons, I. D. H. Oswald, A. Parkin, F. P. A. Fabbiani, J. E. Davidson, A. Dawson, R. E. Aird, et al., *J. Med. Chem.* **2006**, *49*, 6858–6868.

[45] C. M. Clavel, E. Păunescu, P. Nowak-Sliwinska, A. W. Griffioen, R. Scopelliti, P. J. Dyson, *J. Med. Chem.* **2015**, *58*, 3356–3365.

[46] K. J. Kilpin, C. M. Clavel, F. Edafe, P. J. Dyson, *Organometallics* **2012**, *31*, 7031–7039.

[47] S. J. Lucas, R. M. Lord, R. L. Wilson, R. M. Phillips, V. Sridharan, P. C. McGowan, *Dalton Trans* **2012**, *41*, 13800–13802.

[48] R. M. Lord, A. J. Hebden, C. M. Pask, I. R. Henderson, S. J. Allison, S. L. Shepherd, R. M. Phillips, P. C. McGowan, *J Med Chem* **2015**, *58*, 4940–4953.

[49] Z. Almodares, S. J. Lucas, B. D. Crossley, A. M. Basri, C. M. Pask, A. J. Hebden, R. M. Phillips, P. C. McGowan, *Inorg Chem* **2014**, *53*, 727–736.

[50] S. H. van Rijt, A. J. Hebden, T. Amaresekera, R. J. Deeth, G. J. Clarkson, S. Parsons, P. C. McGowan, P. J. Sadler, *J. Med. Chem.* **2009**, *52*, 7753–7764.

[51] R. M. Lord, S. J. Allison, K. Rafferty, L. Ghandhi, C. M. Pask, P. C. McGowan, *Dalton Trans* **n.d.**, *45*, 13196–13203.

[52] S. J. Lucas, R. M. Lord, A. M. Basri, S. J. Allison, R. M. Phillips, A. J. Blacker, P. C. McGowan, *Dalton Trans* **2016**, *45*, 6812–6815.

[53] A. Rodriguez-Barzano, R. M. Lord, A. M. Basri, R. M. Phillips, A. J. Blacker, P. C. McGowan, *Dalton Trans.* **2015**, *44*, 3265–3270.

[54] J. M. Hearn, I. Romero-Canelón, B. Qamar, Z. Liu, I. Hands-Portman, P. J. Sadler, *ACS Chem. Biol.* **2013**, *8*, 1335–1343.

[55] Z. Liu, A. Habtemariam, A. M. Pizarro, G. J. Clarkson, P. J. Sadler, *Organometallics* **2011**, *30*, 4702–4710.

[56] R. Pettinari, F. Marchetti, C. Pettinari, F. Condello, A. Petrini, R. Scopelliti, T. Riedel, P. J. Dyson, *Dalton Trans.* **2015**, *44*, 20523–20531.

[57] M. Erlandsson, V. R. Landaeta, L. Gonsalvi, M. Peruzzini, A. D. Phillips, P. J. Dyson, G. Laurenczy, *Eur J Inorg Chem* **2008**, *2008*, 620–627.

[58] G. Gasser, I. Ott, N. Metzler-Nolte, *J. Med. Chem.* **2011**, *54*, 3–25.

[59] G. Jaouen, A. Vessieres-Jaouen, D. Plazuk, *Ferrocene Derivatives with Anticancer Activity*, Google Patents, **2013**.

[60] P. C. Ford, D. P. Rudd, R. Gaunder, H. Taube, *JACS* **1968**, *90*, 1187–1194.

[61] A. W. Zanella, P. C. Ford, *Inorg Chem* **1975**, *14*, 42–47.

[62] T. Matsubara, P. C. Ford, *Inorg Chem* **1976**, *15*, 1107–1110.

[63] Y. Ilan, H. Taube, *Inorg. Chem.* **1983**, *22*, 1655–1664.

[64] Y. Ilan, M. Kapon, *Inorg. Chem.* **1986**, *25*, 2350–2354.

[65] M. H. Chou, B. S. Brunschwig, C. Creutz, N. Sutin, A. Yeh, R. C. Chang, C. T. Lin, *Inorg. Chem.* **1992**, *31*, 5347–5348.

[66] M. H. Chou, D. J. Szalda, C. Creutz, N. Sutin, *Inorg. Chem.* **1994**, *33*, 1674–1684.

[67] S. M. Redmore, C. E. F. Rickard, S. J. Webb, L. J. Wright, *Inorg. Chem.* **1997**, *36*, 4743–4748.

[68] A. Das, S.-M. Peng, G.-H. Lee, S. Bhattacharya, *New J. Chem.* **2004**, *28*, 712–717.

[69] H. Sigel, R. B. Martin, *Chem. Rev.* **1982**, *82*, 385–426.

[70] A. F. A. Peacock, S. Parsons, P. J. Sadler, *J. Am. Chem. Soc.* **2007**, *129*, 3348–3357.

[71] S. J. Dougan, A. Habtemariam, S. E. McHale, S. Parsons, P. J. Sadler, *Proc. Natl. Acad. Sci.* **2008**, *105*, 11628–11633.

[72] Y. Fu, A. Habtemariam, A. M. Pizarro, S. H. van Rijt, D. J. Healey, P. A. Cooper, S. D. Shnyder, G. J. Clarkson, P. J. Sadler, *J. Med. Chem.* **2010**, *53*, 8192–8196.

[73] J. Y. Qi, L. Q. Qiu, K. H. Lam, C. W. Yip, Z. Y. Zhou, A. S. C. Chan, *Chem. Commun.* **2003**, 1058–1059.

[74] S. Nag, R. J. Butcher, S. Bhattacharya, *Eur J Inorg Chem* **2007**, *2007*, 1251–1260.

[75] M. S. Sanford, J. A. Love, R. H. Grubbs, *J. Am. Chem. Soc.* **2001**, *123*, 6543–6554.

[76] T. J. Seiders, D. W. Ward, R. H. Grubbs, *Org. Lett.* **2001**, *3*, 3225–3228.

[77] A. Seal, S. Ray, *Acta Crystallogr. Sect. C* **1984**, *40*, 929–932.

[78] S. Komeda, G. V. Kalayda, M. Lutz, A. L. Spek, Y. Yamanaka, T. Sato, M. Chikuma, J. Reedijk, *J. Med. Chem.* **2003**, *46*, 1210–1219.

[79] J. A. van Rijn, P. Marques-Gallego, J. Reedijk, M. Lutz, A. L. Spek, E. Bouwman, *Dalton Trans.* **2009**, 10727–10730.

[80] M. Uemura, T. Suzuki, K. Nishio, M. Chikuma, S. Komeda, *Metallomics* **2012**, *4*, 686–692.

[81] V. Brabec, J. Kasparkova, *Drug Resist. Updat.* **2002**, *5*, 147–161.

[82] J. Reedijk, *Proc. Natl. Acad. Sci.* **2003**, *100*, 3611–3616.

[83] D. J. Stewart, *Crit. Rev. Oncol. Hematol.* **2007**, *63*, 12–31.

[84] L. Galluzzi, L. Senovilla, I. Vitale, J. Michels, I. Martins, O. Kepp, M. Castedo, G. Kroemer, *Oncogene* **2012**, *31*, 1869–1883.

[85] J. M. Brown, *Cancer Biol. Ther.* **2002**, *1*, 453–458.

[86] M. Ahmadi, Z. Ahmadihosseini, S. J. Allison, S. Begum, K. Rockley, M. Sadiq, S. Chintamaneni, R. Lokwani, N. Hughes, R. M. Phillips, *Br. J. Pharmacol.* **2014**, *171*, 224–236.

[87] R. M. Phillips, *Cancer Chemother. Pharmacol.* **2016**, *77*, 441–457.

[88] S. B. Reddy, S. K. Williamson, *Expert Opin. Investig. Drugs* **2009**, *18*, 77–87.

[89] Z. Guo, P. J. Sadler, *Angew. Chem. Int. Ed.* **1999**, *38*, 1512–1531.

[90] M. A. Jakupec, M. Galanski, B. K. Keppler, in *Rev. Physiol. Biochem. Pharmacol.*, Springer Berlin Heidelberg, Berlin, Heidelberg, **2003**, pp. 1–53.

[91] V. Brabec, J. Kasparkova, *Drug Resist. Updat.* **2005**, *8*, 131–146.

[92] H. Zorbas, B. K. Keppler, *ChemBioChem* **2005**, *6*, 1157–1166.

[93] J. K.-C. Lau, B. Ensing, *Phys. Chem. Chem. Phys.* **2010**, *12*, 10348–10355.
[94] J. K.-C. Lau, D. V. Deubel, *J. Chem. Theory Comput.* **2006**, *2*, 103–106.
[95] F. Wang, A. Habtemariam, E. P. L. van der Geer, R. Fernández, M. Melchart, R. J. Deeth, R. Aird, S. Guichard, F. P. A. Fabbiani, P. Lozano-Casal, et al., *Proc. Natl. Acad. Sci. U. S. A.* **2005**, *102*, 18269–18274.
[96] A. F. A. Peacock, M. Melchart, R. J. Deeth, A. Habtemariam, S. Parsons, P. J. Sadler, *Chem. – Eur. J.* **2007**, *13*, 2601–2613.
[97] S. Betanzos-Lara, A. Habtemariam, G. J. Clarkson, P. J. Sadler, *Eur. J. Inorg. Chem.* **2011**, *2011*, 3257–3264.
[98] S. Roy, P. U. Maheswari, A. Golobič, B. Kozlevčar, J. Reedijk, *Spec. Issue Met. Med.* **2012**, *393*, 239–245.
[99] P. K. Bhattacharya, S. Dutta, *Indian J Chem* **2003**, *42A*, 268–274.
[100] J. Cosier, A. M. Glazer, *J. Appl. Crystallogr.* **1986**, *19*, 105–107.
[101] Bruker, *APEX2*, Madison, Wisconsin, USA, **2012**.
[102] Agilent, *CrysAlis Pro*, Yarnton, Oxfordshire, England, **2014**.
[103] G. Sheldrick, *Acta Crystallogr. Sect. A* **2008**, *64*, 112–122.
[104] G. M. Sheldrick, T. R. Schneider, in *Methods Enzymol.*, Academic Press, **1997**, pp. 319–343.
[105] G. M. Sheldrick, *SHELXL 2014/7*, University of Göttingen, **2014**.
[106] C. F. Macrae, I. J. Bruno, J. A. Chisholm, P. R. Edgington, P. McCabe, E. Pidcock, L. Rodriguez-Monge, R. Taylor, J. van de Streek, P. A. Wood, *J. Appl. Crystallogr.* **2008**, *41*, 466–470.
[107] M. Thornton-Pett, *WC-A Windown CIF Processor*, **2000**.
[108] A. Spek, *J. Appl. Crystallogr.* **2003**, *36*, 7–13.
[109] O. V. Dolomanov, L. J. Bourhis, R. J. Gildea, J. A. K. Howard, H. Puschmann, *J. Appl. Crystallogr.* **2009**, *42*, 339–341.
[110] P. van der Sluis, A. L. Spek, *Acta Crystallogr. Sect. A* **1990**, *46*, 194–201.